

FIELD VARIATIONAL METHOD IN CALCULATING
ELECTROMAGNETIC SYSTEM PARAMETERS

A thesis presented for the Degree of

Master of Philosophy

of the

University of Southampton

in the

Faculty of Engineering and Applied Science

Department of Electrical Engineering

by

Y.K.H. MUHAMAD FUAD BIN ABDULLAH

December 1981

CONTENTS

Page

ABSTRACT

ACKNOWLEDGEMENTS

LIST OF PRINCIPAL SYMBOLS

CHAPTER ONE

1.1	Introduction	1
1.2	A Method which gives an Upper and a Lower Bound	3

CHAPTER TWO

2.1	Solution of System Differential Equations	6
2.2	Formulation of the Variational Method	7
2.3	Variational Statement in Electrostatic Systems	10
2.4	Energy Functionals in Magnetostatic Systems	14
2.5	Energy Functionals in Static Electromagnetic Systems	15
2.6	Energy Functionals in Resistive Electric Systems	15
2.7	Energy Functional for Eddy-current Type Electromagnetic Systems	16

CHAPTER THREE

3.1	Usefulness of an Improvement Formula	20
3.2	Improvement Formula for Y-Functional	21
3.3	Improvement Formula for Z-Functional	31
3.4	Physical Interpretation of Field Variations in Electrostatics	32

CHAPTER FOUR CALCULATION OF PARAMETERS

4.1	Calculation of Capacitance	37
4.1.1	The upper bound	38
4.1.2	Improvement of upper bound	40
4.1.3	The lower bound of capacitance	42
4.1.4	The improvement of lower bound	44
4.2	Calculation of Inductance	47
4.2.1	The upper bound	48
4.2.2	The lower bound of inductance	51
4.2.3	The improvement of lower bound of inductance	54
4.2.4	Difficulties in calculating the upper bound of inductance	55

4.3	Calculation of Resistance	59
4.3.1	The upper bound	60
4.3.2	The improvement of the upper bound resistance	63
4.3.3	The lower bound of resistance	65
4.3.4	The improvement of lower bound of resistance	66
4.4	The Calculation of Resistance and Reactance of Time-Varying Electromagnetic Systems	68
CHAPTER FIVE THE APPLICATION OF THE FIELD VARIATIONAL METHOD TO MACHINE DESIGN		
5.1	The Slot Description	72
5.2	Calculation of the Lower Bound of Slot Reactance due to the Lower Winding	73
5.3	The Improvement of the Lower Bound of Inductance	78
5.4	Determination of the Upper Bound of Inductance due to the Lower Winding	82
5.5	The Improvement of the Upper Bound	87
5.6	Comparison between Calculated and Test Results	87
5.7	Discussion of Results	88
CHAPTER SIX CONCLUSION		91
APPENDIX I		94
APPENDIX II		98
APPENDIX III		100
APPENDIX IV		109
APPENDIX V		111
APPENDIX VI		115
APPENDIX VII		117
APPENDIX VIII		119

UNIVERSITY OF SOUTHAMPTON

ABSTRACT

FACULTY OF ENGINEERING AND APPLIED SCIENCE

DEPARTMENT OF ELECTRICAL ENGINEERING

Master of Philosophy

FIELD VARIATIONAL METHOD IN CALCULATING
ELECTROMAGNETIC SYSTEM PARAMETERS

by Yeoh Keat Hian Muhamad Fuad bin Abdullah

Variational methods have been used in determining system parameters in a wide range of engineering and physics problems, such as the determination of the resonant frequency, the binding energy, scattering phase shift and the reflection coefficient. The principles involved which are based on the Calculus of Variations are well-established. Examples of the application of the field variational method to some electromagnetic problems are given in this thesis.

The field quantity of an electromagnetic system is varied in such a way that the system energy, whether kinetic, potential or a combination of both, is slightly displaced from its equilibrium. In the case of a purely kinetic energy system, variation of field reduces the system energy. The opposite occurs for the system with purely potential energy. By varying the potential ϕ and the flux density D separately in an electrostatic system, the upper and lower bounds of its capacitance can be calculated. Similarly by varying the magnetic potential ϕ_m and the flux density B , the upper and lower bounds of the system inductance can be calculated. Finally by varying the current density J and the potential ϕ of a resistive electric system, the upper and lower bounds of its resistance can be obtained. Examples of the above three cases of field variation are given.

The results obtained are compared with those already determined elsewhere either analytically or by numerical methods.

The application of the Field Variational Method in the calculation of slot leakage reactance in machine design is shown.

ACKNOWLEDGEMENTS

The author wishes to express his utmost appreciation and thanks to:

Professor P. Hammond, his supervisor, for giving the opportunity to him to do this research as well as for all the encouragement, advice and help given while doing his studies at Southampton University;

Dr. R. L. Stoll for his advice and help rendered especially at times of difficulties in proceeding with the research;

The Central Electricity Generating Board of Britain for the financial support in the form of a studentship;

Messrs. Laurence, Scott and Electromotors Ltd., Norwich, especially to Dr. M. R. Lloyd, for assistance in obtaining useful data;

Miss S. D. Makin for her expert typing of this thesis;

The Government of Malaysia, in particular the Director-General of PWD and the Federal Director of the Electrical Branch of PWD for their kind permission given to do further studies at Southampton University;

Others whose names could not be personally mentioned for various suggestions and assistance;

and last but not least to his wife Majmin whose patience and understanding contributed in no small measure to this thesis.

LIST OF PRINCIPAL SYMBOLS

<u>b</u>	Slot width
<u>c</u>	Slot opening
<u>C</u>	Capacitance
<u>h_1</u>	Depth of conducting region in slot
<u>h_2</u>	
<u>h_3</u>	
<u>h_4</u>	
<u>t</u>	
<u>B</u>	Magnetic flux density
<u>B_1</u>	Initial approximation of magnetic flux density
<u>B_C</u>	Chosen flux density for the improvement of bound
<u>D</u>	Electric flux density
<u>D_1</u>	Initial approximation of electric flux density
<u>D_C</u>	Chosen flux density for the improvement of bound
<u>H</u>	Magnetic field strength
<u>H^*</u>	Complex conjugate of magnetic field strength
<u>J</u>	Current density
<u>J^*</u>	Complex conjugate of current density
<u>L</u>	Inductance
<u>$N\phi$</u>	Total flux linkage
<u>R</u>	Resistance
<u>Y</u>	Convex energy functional
<u>Z</u>	Concave energy functional

ϵ Permittivity
 μ Permeability
 ρ Volume source of electric charge
 ρ_s Surface source of electric charge
 ρ_m Magnetic volume source
 ϕ Electrical potential
 ϕ_s Surface value of electric potential
 ϕ_m Magnetic potential
 ϕ_c Chosen potential for the improvement of bound

CHAPTER ONE1.1 Introduction

The electrical power is no doubt a most important form of power in our present world. Until the 1970's the growth in the electricity demand in the United Kingdom, for example, has been steadily increasing at the rate of 7% per annum doubling every 10 years⁽¹⁾. Corresponding to this growth there has been a parallel increase in the sizes of electrical plants such as transformers, motors, generators and especially so in the case of turbogenerators⁽²⁾. The 500 MW range turbogenerators are nowadays very common at modern power stations and super turbogenerators up to the size of 1200 MW have been built as early as 1973⁽³⁾. As a consequence of such tremendous changes in the sizes of electrical devices, the electrical machinery industry has been becoming more competitive than ever. An accurate prediction of device performance is necessary to meet stringent users' specifications in order that an economical design can be achieved. Tolerances in design are being progressively reduced and optimisation seems to be the rule of the day.

With the advent of large digital computers machine designers have found an indispensable aid in them in achieving optimum designs of their machines. The use of standard software packages has increased in popularity with their sizes becoming larger than ever to meet the users' demands. Silvester has said that finite element packages of the equivalent of 10^4 - 10^5 executable Fortran lines would probably be needed to meet the demands of machine designers in the eighties⁽⁴⁾.

There could arise two main disadvantages from the designer's point of view in using such large standard packages. Firstly, is the possibility of the loss of 'feel' that the designer would possess on his design of a

machine or device. Armed with some basic criteria, a machine designer should always be able to see how the changes in a certain parameter would affect the performance of the machine. Also he should bear in mind the basic assumptions made in the design formulae employed. There is therefore always a possibility that such an insight and 'feel' may be lost when large computer software packages are used in design. More often than not the designer would be given such a massive amount of figure in the computer output that he may likely be lost in trying to extract the relevant and useful information from them. This problem has been largely overcome by the use of post-processors, providing the necessary and required information in the form of graphics and diagrams - even 3-dimensional. Standard packages could be easily adapted to the use of such post-processing methods.

The second possible disadvantage is that the information given by the output of such standard packages would often be more than is required for a particular application; and as such expensive computer time might be wasted in calculating the unwanted information. This is particularly so in the application of finite elements method to electromagnetic field problems. In solving a particular field problem, the finite elements method through discretisation and use of higher order elements, calculates the point values of the field over the whole of the region under consideration. Such information regarding the field at so many points is usually unnecessary if all that is required is the total electromagnetic energy of the region or the associated energy parameter that can express it, for example the resistance, inductance or the capacitance.

The search will certainly go on to find a compromise between the extremes of a totally analytical approach which is very restricted in its

application and a totally numerical approach to electrical design problems. Such a combination of analytical and numerical techniques could overcome to an extent the two disadvantages mentioned above. The field variational method treated in this thesis is one that has this in mind; attempting to utilise fully the analytical advantages offered and keeping to a minimum the amount of computation necessary.

1.2 A Method which gives an Upper and a Lower Bound

An important question one would ask when presented with a numerical solution to a design problem, especially when obtained from the output of a digital computer, would be 'How accurate is it?' or 'How much confidence can we have in it?' In the design of an electrical machine, the designer usually wishes to obtain the equivalent-circuit parameters in the form of resistances and reactances which can help him to specify the performance characteristics of the machine. One would be quite uncertain as to the accuracy of such numerical figures; whether it is on the higher or lower side of the true value. A method of calculation which can give the upper and lower bounds to the true solution would certainly be advantageous. The average of the two bounds would always give a value which is closer to the correct one. We would also be able to know within what limits our estimate of the true value is. The designer would then have the confidence that his design would give the performance characteristics required within some known limits. The uncertainty that might arise from a design parameter without the benefits of an upper and a lower bound can thus be avoided.

The duality⁽⁵⁾ between electric and magnetic fields in terms of moving or stationary sources and expressable in terms of either kinetic or potential energy enables the field variational method to be formulated

so as to give an upper and a lower bound to machine design parameters. This will be shown in the subsequent chapters. Examples of the calculations of upper and lower bounds of capacitance, inductance and resistance are given in Chapter 4. In chapter 5 is given an example of the application of the field variational method in the calculation of the slot leakage reactance of induction motors.

The background to the variational method employed in this thesis can be found in a recently published book entitled 'Energy Methods in Electromagnetism' by P. Hammond. Examples of the calculation of capacitance, inductance and resistance are also found in the said book and in two papers, namely, 'Calculation of inductance and capacitance by means of dual energy principles' and 'Calculation of eddy currents by dual energy methods', both by P. Hammond and J. Penman. The approach to the calculations in this thesis is, however, slightly different in that different energy functionals have been used. Other examples of variational methods applied to electromagnetic systems can be found elsewhere, for example, in the book 'Methods of Theoretical Physics' by Morse and Feshbach, 'Electricity and Magnetism' by E. M. Purcell and 'Computer Techniques for Electromagnetics' edited by R. Mittra. The use of effective slot shapes in slot reactance calculations is a new proposition. A paper based on the material found in Chapter 5 is to be presented at the International Conference on Electrical Machines in Hungary in September 1982 and is given in Appendix VIII.

References

1. LEACH, G. et al : 'A Low Energy Strategy for the U.K.', Science Review Ltd., London. International Institute for Environment and Development (1979), pp 180.
2. LIMMER, R. J. : 'Design Features of Winding Insulation for High Tension Machines', Colloquium paper at Savoy Place, IEE, 16-17 Nov., 1978, London.
3. GARDNER, J. W. : 'New Frontiers in Electricity', GT Foulis & Co. Ltd., Oxfordshire (1973), pp 165.
4. CHARI, M.V.K. and SILVESTER, P. P. : 'Finite Elements in Electrical and Magnetic Field Problems', John Wiley & Sons Ltd., (1980) pp 84.
5. HAGUE, B. : 'The Principles of Electromagnetism - Applied to Electrical Machines', Dover Publications, Inc. N. York (1962), pp 62-65.

CHAPTER TWO2.1 Solution of System Differential Equations

A physical system can be mathematically described by a set of differential equations or a set of integral equations or a combination of both. Maxwell's equations are used to describe the behaviour and characteristics of electromagnetic systems. Maxwell's equations⁽¹⁾ are given by:

$$\underline{\nabla} \times \underline{E} = - \frac{\partial \underline{B}}{\partial t}$$

$$\underline{\nabla} \times \underline{H} = \underline{J} + \frac{\partial \underline{D}}{\partial t}$$

$$\underline{\nabla} \cdot \underline{D} = \rho$$

$$\underline{\nabla} \cdot \underline{B} = 0$$

$$\underline{D} = \epsilon \underline{E}$$

$$\underline{B} = \mu \underline{H} \quad (2.1)$$

In the case of electrostatic systems, the differential equations are given by,

$$\underline{E} = -\underline{\nabla}\phi$$

$$\nabla^2\phi = -\rho/\epsilon \quad \text{where sources are present}$$

$$= 0 \quad \text{where sources are absent} \quad (2.2)$$

For static electromagnetic systems, the equations concerned are

$$\underline{B} = \underline{\nabla} \times \underline{A}$$

$$\underline{\nabla} \cdot \underline{A} = 0$$

$$\nabla^2 \underline{A} = -\mu \underline{J} \quad (2.3)$$

In the case of resistive electric systems, the equations involved are

$$\underline{E} = -\underline{\nabla} \phi$$

$$\underline{\nabla} \cdot \underline{J} = 0$$

$$\underline{J} = \sigma \underline{E} \quad (2.4)$$

One way of solving a set of differential equations is to simultaneously integrate them either analytically or more often numerically. The analytical approach is applicable to only very limited and simple cases. Numerical methods have to be employed in most cases. Another way of solving the differential equations is by means of the variational method based on the calculus of variations.

2.2 Formulation of the Variational Method

Any physical system can be described by a set of differential equations⁽²⁾ given by

$$D(\phi) = 0 \quad (2.5)$$

in the volume v of the system and a set of boundary conditions

$$B(\phi) = 0 \quad (2.6)$$

at the boundary s , where ϕ is an unknown function associated with the system. Alternatively it can be described in the form of a variational principle such that a scalar function I given by

$$I = \int_v L(\phi, \phi', r) dv + \oint_s \ell(\phi, \phi', r) ds \quad (2.7)$$

should be stationary in its first variation, that is,

$$\delta I = \delta \int_v L(\phi, \phi', r) dv + \delta \oint_s \ell(\phi, \phi', r) ds = 0 \quad (2.8)$$

where $L(\phi, \phi', r)$ and $\ell(\phi, \phi', r)$ are some functionals of ϕ, ϕ', r in the region and at the boundary respectively; where ϕ is a function of the space variable r and ϕ' is the first derivative of ϕ with respect to r .

In the rectangular x-y-z coordinate system r is in terms of x, y and z .

When the boundary conditions are satisfied⁽³⁾ such that the second term in equation (2.8) vanishes, corresponding to natural boundary conditions⁽⁴⁾ and permitting variations to occur within the volume only, equation (2.8) can be written simply as

$$\delta \int_v L(\phi, \phi', r) dv = 0 \quad (2.9)$$

This statement is similar to the Hamilton's Principle of Stationary Action,

$$\delta A = \delta \int_{t_1}^{t_2} L dt = 0 \quad (2.10)$$

where the integration is performed with respect to time.

Since equation (2.9) is a variational statement of the system in terms of a scalar functional L over a specified region, it can also be regarded as a virtual displacement of the system⁽⁵⁾. The functional L can be the system potential energy density or its kinetic energy density.

From the theory of the calculus of variations⁽⁶⁾ it can be shown that if equation (2.9) is satisfied at $\phi = \bar{\phi}$ then the following equation is obtained⁽⁷⁾,

$$\left\{ \frac{\partial}{\partial \phi} - \frac{\partial}{\partial \mathbf{r}} \left(\frac{\partial}{\partial \phi'} \right) \right\}_{\bar{\phi}} = 0 \quad (2.11)$$

for the region within v , with the satisfaction of the boundary conditions,

$$B(\phi) = 0 \quad (2.12)$$

Equation (2.11) is called the Euler-Lagrange Differential Equation. The variational principle is called the Euler-Lagrange Variational Principle. See Appendix I for details of the derivation of the Euler-Lagrange Equation.

Conversely if we have equation (2.11) as the differential equation of our physical system, and a variational statement in the form of equation (2.9) can be found, the solution to our system differential equation is given by $\phi = \bar{\phi}$ such that the first variation of the functional I vanishes; that is a stationary⁽⁸⁾ (maximum, minimum or saddle point) value of I is reached. In practice we should be able to identify at which stationary point I is. For example in problems involving I as a functional in terms of potential energy, it is clear that the stationary point of I at equilibrium would be a minimum. Alternatively the second

variation of I can be evaluated to determine the nature of its stationarity.

Many numerical methods associated with variational formulation have been developed. Examples are Moments Methods, the special cases of which are Galerkin's Method and Rayleigh-Ritz Method^(9,10).

2.3 Variational Statement in Electrostatic Systems

The governing physical equations in electrostatic systems are given by,

$$\begin{aligned} \nabla \cdot \underline{D} &= \rho && \text{where sources are present} \\ &= 0 && \text{where sources are absent} \end{aligned} \quad (2.13)$$

$$-\nabla \phi = \underline{E} \quad (2.14)$$

$$\text{and } \underline{D} = \epsilon \underline{E} \quad (2.15)$$

The scalar functional I corresponding to equation (2.7) would be the system energy given either by⁽¹¹⁾,

$$I = \int_v \bar{\rho} \phi - \frac{1}{2\epsilon} |\underline{E}|^2 dv - \int_s \bar{\rho}_s \phi_s ds \quad (2.16)$$

where the variation is performed on the potential ϕ and the volume charge $\bar{\rho}$ and the total boundary charge $\bar{\rho}_s$ are fixed; or

$$I = \int_v \bar{\rho} \phi - \frac{1}{2\epsilon} |\underline{D}|^2 dv - \int_s \rho_s \bar{\phi}_s ds \quad (2.17)$$

where the variation is on the flux density \underline{D} and the volume potential ϕ as well as the boundary potential $\bar{\phi}_s$ fixed.

Alternatively the scalar functional I can be of the form

$$I = \int_v \frac{1}{2\epsilon} |\underline{E}|^2 - \rho \bar{\phi} dv + \oint_s \rho_s \bar{\phi}_s ds \quad (2.18)$$

as in equation (2.16) but with the potential at the point of sources in the volume fixed as well as the boundary surface potential fixed; and

$$I = \int_v \frac{1}{2\epsilon} |\underline{D}|^2 - \bar{\rho} \phi dv + \oint_s \bar{\rho}_s \phi_s ds \quad (2.19)$$

as in equation (2.17) but with the volume charge $\bar{\rho}$ and the total boundary surface charge $\bar{\rho}_s$ kept constant instead.

If there are no charges present in the volume, equations (2.18) and (2.19) can be rewritten simply as,

$$I = \int_v \frac{1}{2\epsilon} |\underline{E}|^2 dv \quad (2.20)$$

$$\text{and } I = \int_v \frac{1}{2\epsilon} |\underline{D}|^2 dv \quad (2.21)$$

as the surface terms vanish. In equation (2.18) where the variation is performed on the potential ϕ , fixing of surface potential fixes the surface potential energy. Similarly in equation (2.19) where variation is performed on the flux density, fixing of surface charge $\bar{\rho}_s$ fixes the surface energy too. The closed-loop integral of each becomes zero. In these two cases, the volume sources are absent and hence are only implicitly expressed through the field quantities.

Following the nomenclature used in reference (12) where Y denotes a convex energy functional having a minimum and Z a concave functional with a maximum, equations (2.16), (2.17), (2.20) and (2.21) can be written as

$$Z = \int_V \bar{\rho}\phi - \frac{1}{2}\epsilon |\underline{E}|^2 dv - \oint_S \bar{\rho}_S \phi_S ds \quad (2.22)$$

$$Z = \int_V \rho\bar{\phi} - \frac{1}{2\epsilon} |\underline{D}|^2 dv - \oint_S \rho_S \bar{\phi}_S ds \quad (2.23)$$

$$Y = \int_V \frac{1}{2} \epsilon |\underline{E}|^2 dv \quad (2.24)$$

$$Y = \int_V \frac{1}{2\epsilon} |\underline{D}|^2 dv \quad (2.25)$$

There are therefore four possible variations which can be performed on an electrostatic system governed by equations (2.13) and (2.14). The variations in the system potential ϕ with the energy functionals concerned being given by equations (2.22) and (2.24), give an upper bound and a lower bound of parameter value. Similarly the variations in the flux density \underline{D} with the energy functionals given by equations (2.23) and (2.25), give another pair of upper and lower bounds; so do the two Y -functionals. Altogether there are four possible pairs of upper and lower bounds. The determination of the upper and lower bounds considered in this thesis is by using the 2 Y -functionals given by equations (2.24) and (2.25).

At equilibrium we have the variational statements

$$\delta Y = 0 \quad (2.26)$$

for the case of the system whose energy is expressed in the form of potential energy and

$$\delta Z = 0 \quad (2.27)$$

when the system energy is expressed as kinetic energy.

In the Y-functionals the system sources are implicit whereas in the Z-functionals the system sources are explicitly expressed. By implicit it is meant that the sources of the field are being incorporated in the expression of the field itself as in equation (2.24) and (2.25). On the other hand, equations (2.22) and (2.23) have the sources of the fields expressed in them to account for the energy contributed towards the overall system energy. The Y and Z functionals for other electromagnetic systems can be similarly obtained.

As a check, equation (2.11) can be applied to equations (2.22), (2.23), (2.24) and (2.25) to show that the Euler-Lagrange Equations associated with them are given by the same system equations of (2.13) and (2.14). See Appendix II for details.

The approach to the variational formulation in electrostatic systems given in reference (11) is slightly different in that the author's argument starts with the statement of the principle of virtual work. The possibility of integrating this statement would give rise to the required variational statement.

2.4 Energy Functionals in Magnetostatic Systems (In the absence of current within the region of interest)

The differential equations of magnetostatic systems are given by,

$$\underline{\nabla} \times \underline{H} = 0 \quad (2.28)$$

$$-\underline{\nabla} \phi_m = \underline{H} \quad (2.29)$$

$$\underline{\nabla} \cdot \underline{B} = \rho_m \quad \text{if sources are present}$$

$$= 0 \quad \text{if sources are absent} \quad (2.30)$$

The energy functionals corresponding to equations (2.22), (2.23), (2.24) and (2.25) can be obtained for magnetostatic systems as well.

These are

$$Z = \int_v \rho_m \phi_m - \frac{1}{2\mu} |\underline{H}|^2 dv - \int_s \rho_{ms} \phi_{ms} ds \quad (2.31)$$

$$Z = \int_v \rho_m \bar{\phi}_m - \frac{1}{2\mu} |\underline{B}|^2 dv - \int_s \rho_{ms} \bar{\phi}_{ms} ds \quad (2.32)$$

$$Y = \int_v \frac{1}{2\mu} |\underline{H}|^2 dv \quad (2.33)$$

$$Y = \int_v \frac{1}{2\mu} |\underline{B}|^2 dv \quad (2.34)$$

What has been said for the electrostatic systems as to the behaviour of the Y and Z-functionals still applies to the magnetostatic systems.

2.5 Energy Functionals in Static Electromagnetic Systems

The system equations of static electromagnetic systems are given by

$$\underline{\nabla} \times \underline{H} = \underline{J} \quad (2.35)$$

$$\underline{\nabla} \cdot \underline{B} = 0 \quad (2.36)$$

$$\underline{\nabla} \times \underline{A} = \underline{B} \quad (2.37)$$

The Y and Z functionals can be found and are given by

$$Z = \int_v \underline{J} \cdot \underline{A} - \frac{1}{2\mu} |\underline{H}|^2 dv - \oint_s \underline{J}_s \cdot \underline{H}_s ds \quad (2.38)$$

$$Z = \int_v \underline{J} \cdot \underline{A} - \frac{1}{2\mu} |\underline{B}|^2 dv - \oint_s \underline{J}_s \cdot \underline{H}_s ds \quad (2.39)$$

$$Y = \int_v \frac{1}{2} |\underline{H}|^2 dv \quad (2.40)$$

$$Y = \int_v \frac{1}{2\mu} |\underline{B}|^2 dv \quad (2.41)$$

2.6 Energy Functionals in Resistive Electric Systems

For the case of resistive systems the governing system equations are given by,

$$\underline{\nabla} \times \underline{E} = 0 \quad (2.42)$$

$$-\underline{\nabla}\phi = \underline{E} \quad (2.43)$$

$$\underline{J} = \sigma \underline{E} \quad (2.44)$$

The energy functionals for resistive systems are^(13,14)

$$Z = - \int_v \frac{b}{2\sigma} |\underline{J}|^2 dv - \oint_s b(\bar{\phi}_s \underline{J}_s) ds \quad (2.45)$$

$$Z = - \int_v \frac{\sigma b}{2} |\underline{E}|^2 dv - \oint_s b(\phi_s \bar{\underline{J}}_s) ds \quad (2.46)$$

$$Y = \int_v \frac{b}{2\sigma} |\underline{J}|^2 dv \quad (2.47)$$

$$Y = \int_v \frac{\sigma b}{2} |\underline{E}|^2 dv \quad (2.48)$$

2.7 Energy Functional for Eddy-current Type Electromagnetic Systems

The above time dependent electromagnetic systems have functionals which are expressed in terms of complex quantities and their conjugates. The complex conjugate quantities are necessary in order that such time-varying systems may be made independent of time in as far as defining the system energy is concerned. The system differential equations are given by,

$$\underline{\nabla} \times \underline{H} = \underline{J} \quad (2.49)$$

$$\underline{\nabla} \times \underline{E} = - \frac{\partial \underline{B}}{\partial t} \quad (2.50)$$

$$\underline{J} = \sigma \underline{E} \quad (2.51)$$

$$\underline{B} = \mu \underline{H} \quad (2.52)$$

and the energy functionals are given by⁽¹³⁾,

$$Z = - \int_V \frac{\sigma}{2} (\underline{E} \cdot \underline{E}^*) + \frac{j\omega}{2\mu} (\underline{B} \cdot \underline{B}^*) dv - \oint_S (\underline{E} \times \underline{H}^*) \cdot \hat{\underline{n}} ds \quad (2.53)$$

$$Z = - \int_V \frac{\sigma}{2} (\underline{E} \cdot \underline{E}^*) + \frac{j\omega}{2\mu} (\underline{B} \cdot \underline{B}^*) dv \quad (2.54)$$

$$Y = \int_V \frac{1}{2\sigma} (\underline{J} \cdot \underline{J}^*) + \frac{j\omega\mu}{2} (\underline{H} \cdot \underline{H}^*) dv + \oint_S (\underline{E} \times \underline{H}^*) \cdot \hat{\underline{n}} ds \quad (2.55)$$

$$Y = \int_V \frac{1}{2\sigma} (\underline{J} \cdot \underline{J}^*) + \frac{j\omega\mu}{2} (\underline{H} \cdot \underline{H}^*) dv \quad (2.56)$$

The use of the conjugate functions can be illustrated as follows.

Let us use equation (2.56) above as the example. The current density can be expressed as

$$\underline{J} = J e^{j\omega t} \quad (2.57)$$

where ω is the frequency and t time in seconds.

The complex conjugate is therefore given by,

$$\underline{J}^* = J e^{-j\omega t} \quad (2.58)$$

The product of equation (2.57) and (2.58) is,

$$\begin{aligned} \underline{J} \cdot \underline{J}^* &= J e^{j\omega t} \cdot J e^{-j\omega t} \\ &= J^2 \\ &= |\underline{J}|^2 \end{aligned} \quad (2.59)$$

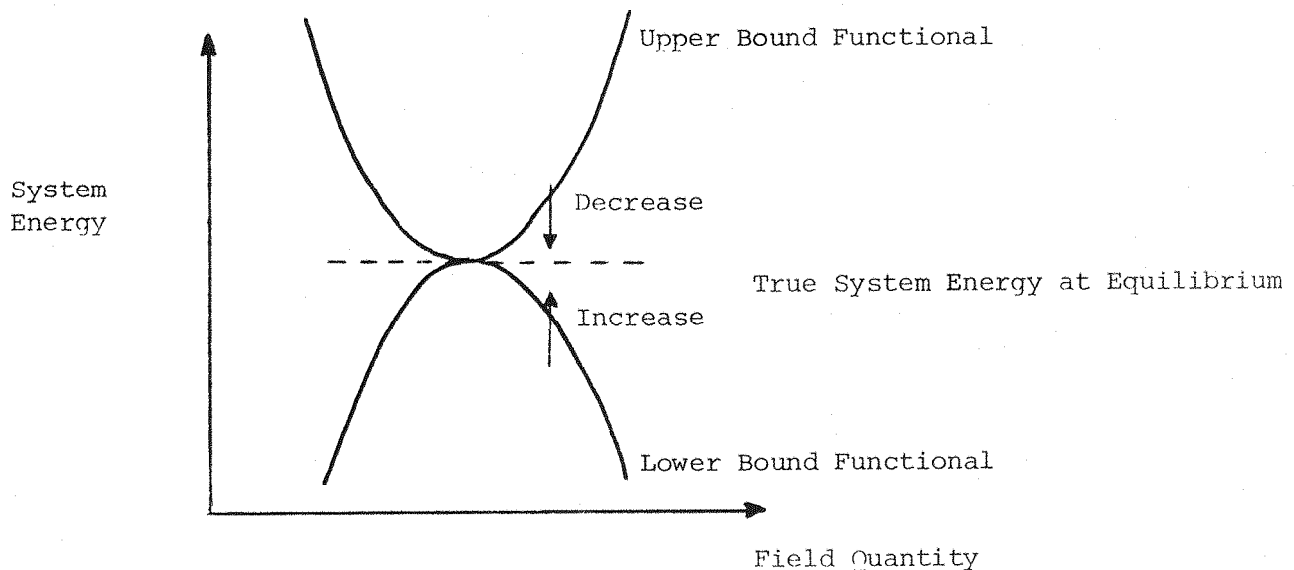
The use of the complex conjugate functions is seen to have made the time-varying current density \underline{J} become independent of time as shown above. Equation (2.59) can be compared with the energy functional in terms of $|\underline{J}|^2$ expressed in equation (2.47).

References

1. HAMMOND, P. : 'Applied Electromagnetism', Pergamon Press, Oxford (1971), pp 373.
2. ZIENKIEWICZ, O. C. : 'Finite Elements - The Basic Concepts and an Application to 3-D Magnetostatic Problems' in the book 'Finite Elements in Electrical and Magnetic Field Problems' edited by MVK Chari and PP Silvester, John Wiley & Sons Ltd., (1980), pp 12.
3. SAGAN, H. : 'Boundary and Eigenvalue Problems in Mathematical Physics', John Wiley & Sons Inc., N. York (1961), pp 28-31.
4. LANCZOS, C. : 'The Variational Principle of Mechanics', University of Toronto Press (1949), pp 68-73.
5. McIVER, D. B. : 'Back to Virtual Power', paper presented at International Conference on Variational Methods in Engineering at Southampton University on 25-9-72, pg. 1/65 in 'Variational Methods in Engineering Vol. I', edited by C. A. Brebbia and H. Tottenham, Southampton University Press (1973).
6. LANCZOS, C. : 'The Variational Principle of Mechanics', University of Toronto Press (1949), pp 54-60.
7. ARTHURS, A. M. : 'Complementary Variational Principles', Clarendon Press, Oxford (1970), pp 2-3.
8. MORSE, P. M. and FESHBACH, H. : 'Methods of Theoretical Physics', McGraw-Hill Co. New York (1953), pp 1107.
9. HARRINGTON, R. F. : 'Field Computation by Moment Methods', MacMillan Co. N. York (1968), pp 5-20.
10. SAGAN, H. : 'Boundary and Eigenvalue Problems in Mathematical Physics', John Wiley & Sons, N. York (1961), pp 273-286.
11. HAMMOND, P. : 'Energy Methods in Electromagnetism', Clarendon Press, Oxford (1981), pp 58-60.
12. HAMMOND, P. and PENMAN, J. : 'Calculation of Inductance and Capacitance by Means of Dual Energy Principles', Proc. IEE, 1976, 123(6), pp 554-559.
13. HAMMOND, P. and PENMAN, J. : 'Calculation of Eddy Currents by Dual Energy Methods', Proc. IEE, Vol. 125(7), July 1978, pp 701-708.
14. HAMMOND, P. : 'Energy Methods in Electromagnetism', Clarendon Press, Oxford (1981), pp 122-127.

CHAPTER THREE3.1 Usefulness of an Improvement Formula

When calculating a bound for a parameter of interest it is helpful to have a way of improving this bound so as to get closer to the true value. This means the increasing of the lower bound and decreasing the upper bound. See Figure 1.

Figure 1 System Energy Functionals

Two obvious advantages are immediately seen in that while enabling a better answer to be obtained, we are at the same time able to check that the improved value does not overshoot and cross-over the other bound. For example the improved value of the lower bound should not be higher than the value of the upper bound.

3.2 Improvement Formula for Y-Functional

Consider the electrostatic system having the energy given by equation (2.25),

$$Y = \int_V \frac{1}{2\epsilon} |\underline{D}|^2 dv \quad (3.1)$$

As explained in section 2.3 the variation that could be performed on this system is the variation in the flux density \underline{D} with the quantity of surface charge remaining unaltered in the process. The Y-functional is a convex functional having a minimum.

Let \underline{D}_1 be the flux density such that it is the solution of the Euler-Lagrange equation minimising equation (3.1), then it would be a good approximation of the flux density of the electrostatic system. \underline{D}_1 is a function of the space variables. The energy due to \underline{D}_1 would be,

$$Y_1 = \int_V \frac{1}{2\epsilon} |\underline{D}_1|^2 dv \quad (3.2)$$

If \underline{D}_1 is varied to \underline{D}_2 by a small amount $\alpha \underline{D}_c$, we have

$$\underline{D}_2 = \underline{D}_1 + \alpha \underline{D}_c \quad (3.3)$$

where α is an arbitrary constant and \underline{D}_c a suitably chosen expression of the flux density.

The electrostatic energy of the system due to \underline{D}_2 would be,

$$Y_2 = \int_V \frac{1}{2\epsilon} |\underline{D}_2|^2 dv \quad (3.4)$$

$$\begin{aligned}
 &= \int_v \frac{1}{2\epsilon} |\underline{D}_1 + \alpha \underline{D}_C|^2 dv \\
 &= \int_v \frac{1}{2\epsilon} \{ |\underline{D}_1|^2 + 2\alpha \underline{D}_1 \cdot \underline{D}_C + \alpha^2 |\underline{D}_C|^2 \} dv
 \end{aligned} \tag{3.4}$$

Minimising Y_2 with respect to α ; we obtain,

$$\begin{aligned}
 \frac{\partial Y_2}{\partial \alpha} = 0 &= \int_v \frac{1}{\epsilon} \{ \underline{D}_1 \cdot \underline{D}_C + \alpha |\underline{D}_C|^2 \} dv \\
 \therefore \alpha &= - \frac{\int_v \frac{1}{\epsilon} \underline{D}_1 \cdot \underline{D}_C dv}{\int_v \frac{1}{\epsilon} |\underline{D}_C|^2 dv}
 \end{aligned} \tag{3.5}$$

Putting equation (3.5) into equation (3.4) gives,

$$Y_2 = \int_v \frac{1}{2\epsilon} |\underline{D}_1|^2 dv - \frac{\frac{1}{2} \left[\int_v \frac{1}{\epsilon} \underline{D}_1 \cdot \underline{D}_C dv \right]^2}{\int_v \frac{1}{\epsilon} |\underline{D}_C|^2 dv} \tag{3.6}$$

Comparing with equation (3.2), equation (3.6) can be written as,

$$Y_2 = Y_1 - \frac{\frac{1}{2} \left[\int_v \frac{1}{\epsilon} \underline{D}_1 \cdot \underline{D}_C dv \right]^2}{\int_v \frac{1}{\epsilon} |\underline{D}_C|^2 dv} \tag{3.7}$$

Equation (3.7) shows that there is a reduction in the value of functional Y_1 and remembering that a reduction means a closer value to

the correct system energy, we thus have an improvement scheme for the initial approximation of flux density \underline{D}_1 . Figure 2 will make this clearer.

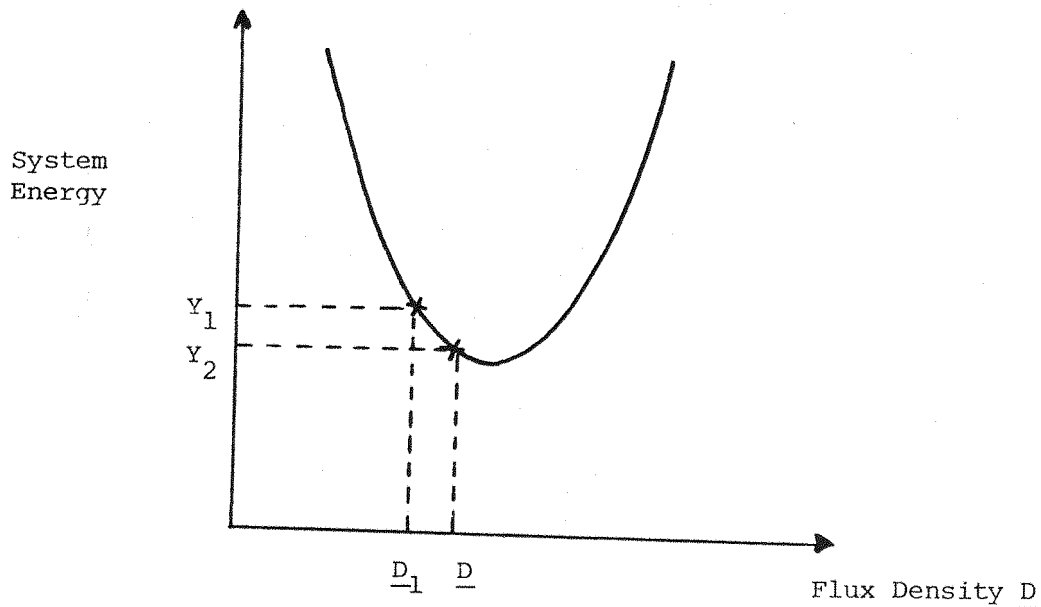


Figure 2 Improvement of Functional Value

The choice of the flux density \underline{D}_c depends on two conditions.

Firstly consider the boundary conditions of the flux densities \underline{D}_1 and \underline{D}_2 . From equation (3.3), remembering that we are keeping the total surface charge constant, we have at the boundary,

$$\oint_S \underline{D}_2 \cdot d\underline{s} = \oint_S \underline{D}_1 \cdot d\underline{s} \quad (3.8)$$

For this to be true we have at the boundary the condition that

$$\oint_S \alpha \underline{D}_c \cdot d\underline{s} = 0 \quad (3.9)$$

Since α is arbitrary and can assume any value, we have as one of the conditions of \underline{D}_c ,

$$\oint_S \underline{D}_c \cdot d\underline{s} = 0 \quad (3.10)$$

The other condition which \underline{D}_c has to satisfy is in the volume of the system. The addition of $\alpha \underline{D}_c$ to \underline{D}_1 should not alter the system under consideration. No new sources can be introduced. Therefore we have over the whole region,

$$\nabla \cdot \underline{D}_2 = \nabla \cdot \underline{D}_1 \quad (3.11)$$

and comparing with equation (3.3), this implies that the condition for \underline{D}_c is

$$\nabla \cdot \alpha \underline{D}_c = 0 \quad (3.12)$$

Since α is an arbitrary constant, the condition \underline{D}_c needs to satisfy is simply,

$$\nabla \cdot \underline{D}_c = 0 \quad (3.13)$$

The choice of \underline{D}_c for this improvement scheme therefore must be such that it satisfies both equations (3.10) and (3.13).

Similar arguments can be made for the Y-functional given by equation (2.24), that is,

$$Y = \int_V \frac{1}{2} \epsilon |\underline{E}|^2 dv \quad (3.14)$$

As stated in section 2.3 the field quantity to be varied in this case is the volume potential ϕ with the surface potential being kept constant. Corresponding to equations (3.2), (3.3), (3.4) and (3.5) above we have for this case,

$$Y_1 = \int \frac{1}{2} \epsilon |\underline{E}_1|^2 dv = \int \frac{1}{2} \epsilon |\nabla \phi_1|^2 dv \quad (3.15)$$

$$\phi_2 = \phi_1 + \alpha \phi_c \quad (3.16)$$

$$Y_2 = \int_v \frac{1}{2} \epsilon \left\{ |\underline{E}|^2 + 2\alpha \underline{E}_1 \cdot \underline{E}_c + \alpha^2 |\underline{E}_c|^2 \right\} dv \quad (3.17)$$

and

$$\alpha = - \frac{\int_v \epsilon \underline{E}_1 \cdot \underline{E}_c dv}{\int_v \epsilon |\underline{E}_c|^2 dv} \quad (3.18)$$

The functional Y_2 is now given by,

$$Y_2 = Y_1 - \frac{\frac{1}{2} \left[\int_v \epsilon \underline{E}_1 \cdot \underline{E}_c dv \right]^2}{\int_v \epsilon |\underline{E}_c|^2 dv} \quad (3.19)$$

In this case the boundary potential is fixed and from equation (3.16), we have, at the boundary,

$$\phi_2 = \phi_1 \quad (3.20)$$

which implies that,

$$\alpha \phi_c = 0 \quad \text{at the boundary.} \quad (3.21)$$

Since α is an arbitrary constant, we have the condition that ϕ_c should vanish at the boundary. The volume condition for ϕ_c corresponding to equation (3.13) requiring no new sources to be introduced is given by,

$$\underline{\nabla} \cdot \underline{\nabla} \phi_c = 0$$

$$\text{or } \nabla^2 \phi_c = 0 \quad (3.22)$$

The conditions for the choice of D_c given by equations (3.10) and (3.13) can be proven as follows. If the true system energy is Y given by flux density D , then any variation of the flux density from D to D_1 would cause an increase in the energy from Y to Y_1 . See Figure 3.

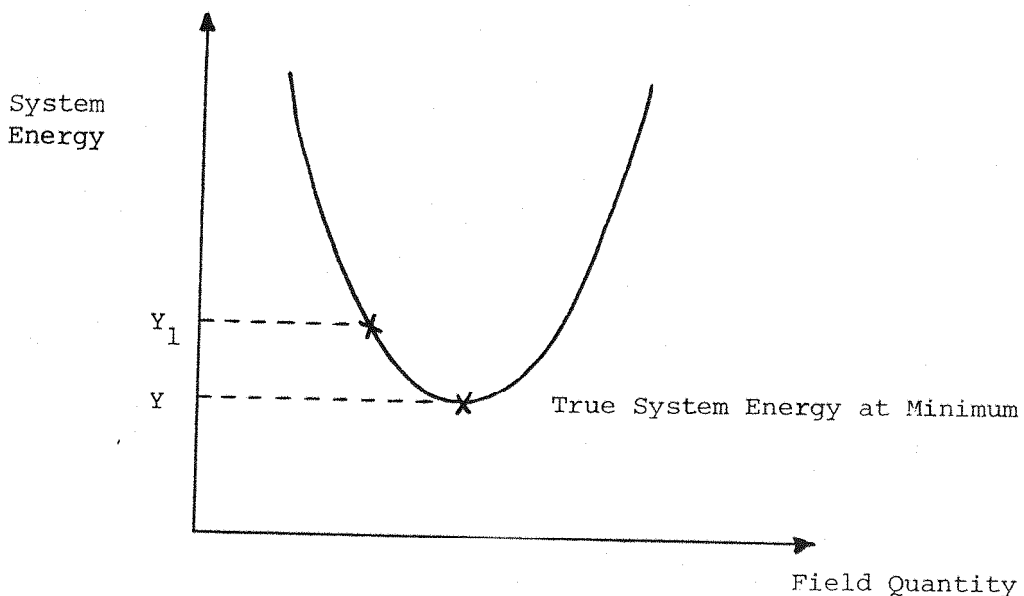


Figure 3 Approximated System Energy Y_1

The change in energy is given by

$$\begin{aligned}
 Y_1 - Y &= \int_v \frac{1}{2\epsilon} |\underline{D}_1|^2 dv - \int_v \frac{1}{2\epsilon} |\underline{D}|^2 dv \\
 &= \int_v \frac{1}{2\epsilon} (\underline{D}_1 - \underline{D})^2 dv + \int_v \frac{1}{\epsilon} \underline{D} \cdot (\underline{D}_1 - \underline{D}) dv
 \end{aligned} \tag{3.23}$$

Substituting $\underline{D} = \epsilon \underline{E} = -\epsilon \nabla \phi$ we can write the second term on the right hand side as

$$\int_v \frac{1}{\epsilon} \underline{D} \cdot (\underline{D}_1 - \underline{D}) dv = - \int_v \nabla \phi \cdot (\underline{D}_1 - \underline{D}) dv \tag{3.24}$$

The Divergence Theorem can be written as,

$$\begin{aligned}
 \int_v \nabla \cdot (\phi \underline{D}) dv &= \oint_s \phi_s \underline{D} \cdot \underline{ds} \\
 \text{or } \int_v \phi (\nabla \cdot \underline{D}) + \nabla \phi \cdot \underline{D} dv &= \oint_s \phi_s \underline{D} \cdot \underline{ds}
 \end{aligned} \tag{3.25}$$

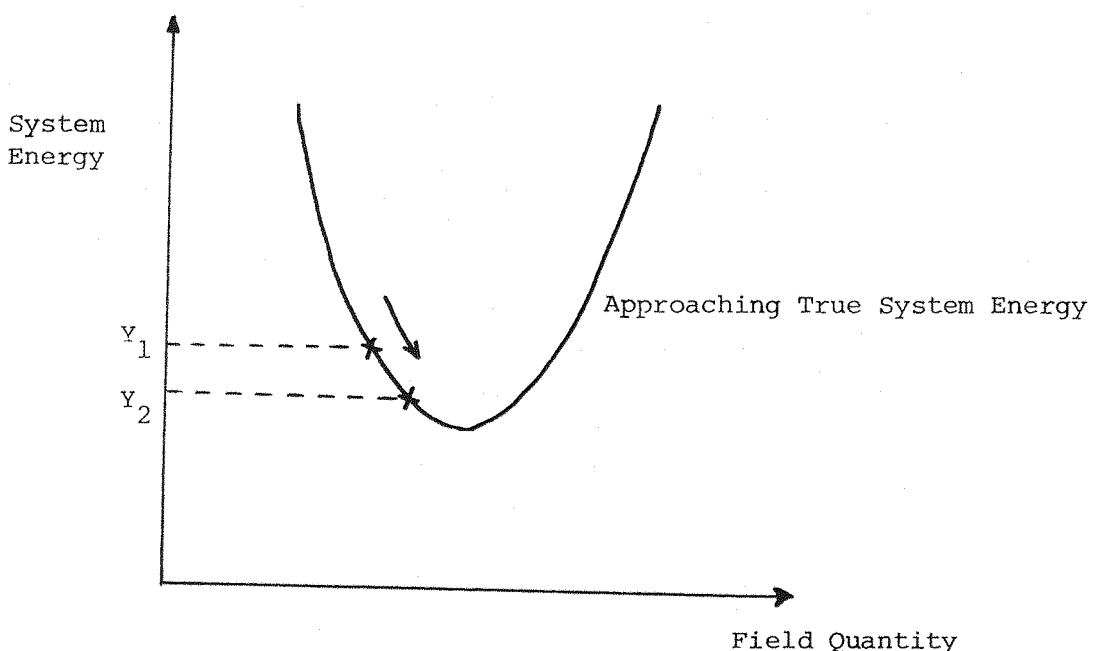


Figure 4 Improvement on Energy Y_1

By using the Divergence Theorem, equation (3.24) becomes,

$$-\int_v \nabla \phi \cdot (\underline{D}_1 - \underline{D}) dv = -\oint_s \phi_s (\underline{D}_1 - \underline{D}) \cdot d\underline{s} + \int_v \phi \nabla \cdot (\underline{D}_1 - \underline{D}) dv \quad (3.26)$$

Equation (3.23) can now be written in terms of equations (3.24) and (3.26),

$$Y_1 - Y = \int_v \frac{1}{2\epsilon} |\underline{D}_1 - \underline{D}|^2 dv + \int_v \phi \nabla \cdot (\underline{D}_1 - \underline{D}) dv - \oint_s \phi_s (\underline{D}_1 - \underline{D}) \cdot d\underline{s} \quad (3.27)$$

For Y_1 to be always higher than the true system energy Y for all possible variations in the flux density, we should have the conditions,

$$\int_v \phi \nabla \cdot (\underline{D}_1 - \underline{D}) dv = 0 \quad \text{in the volume} \quad (3.28)$$

and

$$\oint_s \phi_s (\underline{D}_1 - \underline{D}) \cdot d\underline{s} = 0 \quad \text{at the boundary} \quad (3.29)$$

This means that for arbitrary values of ϕ in the volume the divergence of the variation $(\underline{D}_1 - \underline{D})$ should always be zero; implying that no new sources should be introduced in the variation of the flux density. This condition can be compared with equation (3.13).

For a constant potential at the boundary surface, it being a conductor, equation (3.29) becomes,

$$\oint_s \phi_s (\underline{D}_1 - \underline{D}) \cdot d\underline{s} = \phi_s \oint_s (\underline{D}_1 - \underline{D}) \cdot d\underline{s} \quad (3.30)$$

For this to be zero, the necessary condition at the boundary is that the total charge at the boundary surface remains constant in the variation. This condition is similar to equation (3.10).

Therefore, if we have a system energy Y_1 approximated by using the flux density D_1 , and an improved system energy Y_2 due to D_2 (see Figure 4), we can write equation (3.27) as

$$Y_1 - Y_2 = \int_v \frac{1}{2\epsilon} (D_1 - D_2)^2 dv + \int_v \phi \nabla \cdot (D_1 - D_2) dv - \oint_s \phi_s (D_1 - D_2) \cdot ds \quad (3.31)$$

For improvement to be possible equation (3.31) must always be positive and the necessary conditions are those given by equation (3.18) and (3.13) if we write,

$$(D_1 - D_2) = -\alpha D_c \quad (3.32)$$

where α is an arbitrary constant and D_c the variation of the flux density.

The conditions for the choice of ϕ_c can similarly be proven in the manner shown for D_c . If the true system energy Y due to ϕ be varied to Y_1 due to the variation in the potential to ϕ_1 , (see Figure 3) we have the change in the system energy given by,

$$Y_1 - Y = \int_v \frac{1}{2} \epsilon |\nabla \phi_1|^2 dv - \int_v \frac{1}{2} \epsilon |\nabla \phi|^2 dv = \int_v \frac{1}{2} \epsilon |\nabla \phi_1 - \nabla \phi|^2 dv + \int_v \epsilon \nabla \phi \cdot (\nabla \phi_1 - \nabla \phi) dv \quad (3.33)$$

By using the divergence theorem of equation (3.25), we can write the second term on the right hand side of equation (3.33) as

$$\begin{aligned} \int \epsilon \underline{\nabla} \phi \cdot (\underline{\nabla} \phi_1 - \underline{\nabla} \phi) dv &= \int \epsilon \underline{\nabla} \phi \cdot \underline{\nabla} (\phi_1 - \phi) dv \\ &= \oint_s \epsilon (\phi_1 - \phi)_s \underline{\nabla} \phi \cdot \underline{ds} - \int_v \epsilon (\phi_1 - \phi) \cdot \nabla^2 \phi dv \end{aligned} \quad (3.34)$$

Equation (3.33) can now be written as,

$$\begin{aligned} Y_1 - Y &= \int_v \frac{1}{2} \epsilon |\underline{\nabla} \phi_1 - \underline{\nabla} \phi|^2 dv + \oint_s \epsilon (\phi_1 - \phi)_s \underline{\nabla} \phi \cdot \underline{ds} \\ &\quad - \int_v \epsilon (\phi_1 - \phi) \nabla^2 \phi dv \end{aligned} \quad (3.35)$$

For Y_1 to be always higher for all possible variations of the potential, we need the right hand side equation (3.35) to be always positive. Thus the conditions necessary for this to be achieved are,

$$\int_v \epsilon (\phi_1 - \phi) \nabla^2 \phi dv = 0 \quad \text{in the volume} \quad (3.36)$$

and $\oint_s \epsilon (\phi_1 - \phi)_s \underline{\nabla} \phi \cdot \underline{ds} = 0 \quad \text{at the boundary} \quad (3.37)$

For any arbitrary variation in the potential $(\phi_1 - \phi)$, we require that $\nabla^2 \phi = 0$ implying that there should be no volume sources in the system. At the boundary we require that the potential be fixed such that there is no variation and thus requiring that $(\phi_1 - \phi)_s = 0$.

Therefore if we have a system energy Y_1 and need to improve it to Y_2 (see Figure 4), we can write equation (3.35) as,

$$Y_1 - Y_2 = \int_v \frac{1}{2} \epsilon |\nabla \phi_1 - \nabla \phi_2|^2 dv + \oint_s \epsilon (\phi_1 - \phi_2) s \nabla \phi_2 \cdot ds$$

$$- \int_v \epsilon (\phi_1 - \phi_2) \nabla^2 \phi_2 dv \quad (3.38)$$

For improvement to take place for any variation in potential equation (3.38) must always be positive and the necessary condition are those given by equations (3.21) and (3.22) if we write

$$(\phi_1 - \phi_2) = - \alpha \phi_c \quad (3.39)$$

where α is an arbitrary constant and ϕ_c the variation in potential.

The volume condition of $\nabla^2 \phi_c = 0$ is however not strictly required as will be demonstrated by examples in Chapter 4, so long as the boundary condition $\phi_c = 0$ is satisfied. The potential being scalar means that it can be easily handled mathematically in contrast with variations involving vector quantities as in the case of flux density D . This is an advantage of using the scalar potential variation. The sources which might be introduced do not seem to invalidate the improvement scheme when it is applied to all the examples in Chapter 4.

3.3 Improvement Formula for Z-Functional

The improvement formula for the Z-functional is not as easy to obtain as that for the Y-functional. In this case we need a scheme which would increase the system energy for improvement to take place. The simple procedure shown in the last section does not apply easily

to the Z-functional due to the explicit presence of the system sources as well as the presence of the surface energy term.

This is however not a serious disadvantage in the application of the field variational method to determining system parameters as will be shown in Chapters 4 and 5.

3.4 Physical Interpretation of Field Variations in Electrostatics

As mentioned in section 2.3, there are four possible field variations for an electrostatic system described by the system differential equations (2.13) and (2.14). The types of variations are:

1. Variation in volume potential ϕ with total boundary charge ρ_s kept constant and the volume charge ρ fixed.
2. Variation in volume potential ϕ with boundary potential ϕ_s fixed in the absence of the volume charge ρ .
3. Variation in volume flux density D with total boundary charge ρ_s remaining constant in the absence of the volume charge ρ .
4. Variation in volume flux density D with boundary potential ϕ_s and the volume potential ϕ fixed.

The variation in the volume potential ϕ can be achieved physically by inserting a conducting sheet of negligible thickness. The conducting sheet forms into an equipotential surface in the volume. In the case where the quantity of surface charge is kept constant and the volume charge sources fixed with only the volume potential varied by the insertion of such conducting sheets, there is a decrease in the system energy caused by the work done by the fixed charges in drawing the conducting sheets into the system. This variation corresponds to the Z-functional of equation (2.22),

$$Z = \int_v \bar{\rho} \phi - \frac{1}{2} \epsilon |\underline{E}|^2 dv - \oint_s \bar{\rho}_s \phi_s ds \quad (3.40)$$

If the volume potential is varied by keeping the boundary potential ϕ_s constant and in the absence of volume sources we have an increase in the system energy caused by the work done in inserting the thin conducting sheets into the volume. This variation corresponds to the Y-functional of equation (2.24),

$$Y = \int_v \frac{1}{2} \epsilon |\underline{E}|^2 dv \quad (3.41)$$

We remember that in this case the sources of the system are implicit as against the explicit nature of sources in the previous case.

The variation of flux density \underline{D} can be physically achieved by the insertion of very thin flux barriers.

They are placed along the flux lines varying the shapes of flux tubes.

If flux barriers are inserted into an electrostatic system with the total surface charge ρ_s kept constant, we have an increase in the system energy caused by the work done in inserting the flux barriers into the system.

The Y-functional corresponding to this variation is given by equation (2.25),

$$Y = \int_v \frac{1}{2\epsilon} |\underline{D}|^2 dv \quad (3.42)$$

If, however, the variation in \underline{D} is performed by fixing the boundary potential ϕ_s , as well as the volume potential, there would be an exchange in energy between the fixed potential and the flux barriers causing a decrease in the system energy proportional to the second order variation of \underline{D} .

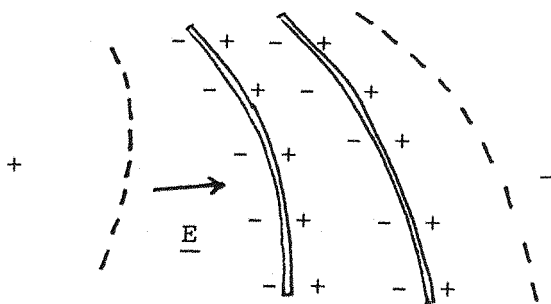


Figure 5 Conducting Sheets or Double Layers of Charge

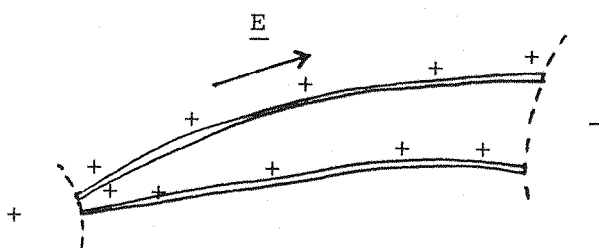


Figure 6 Flux Barriers or Insulating Sheets

The Z-functional corresponding to this type of variation is given by equation (2.23),

$$Z = \int_v \rho \bar{\phi} - \frac{1}{2\epsilon} |\underline{D}|^2 dv - \oint_s \rho_s \bar{\phi}_s ds \quad (3.43)$$

The above four types of field variations cause increase or decrease in the system energy which is proportional to the second order variations of the field.

Other types of field variation which involve the insertion of conducting sheets and flux barriers that are not negligible in thickness and volume are possible and are given in reference (1). They are however not purely of the second order type mentioned above.

The concepts of conducting sheets and flux barriers can be extended to include other electromagnetic systems. We have magnetic flux barriers and infinitely permeable sheets in magnetostatic systems and current barriers and conducting sheets in resistive electric systems.

Reference

1. HAMMOND, P. : 'Energy Methods in Electromagnetism', Clarendon Press, Oxford (1981), pp 100-101.

CHAPTER FOURCALCULATION OF PARAMETERS

The calculations of the upper and lower bounds of parameters namely capacitance, inductance and resistance by the approach using the 2-Y functionals are shown in this chapter using simple configurations.

4.1 Calculation of Capacitance

The example used is the configuration shown in Figure 7 where a square tubing has its inner surface fixed at a potential of V volts and the outer surface at 0 volts. We shall calculate the capacitance per unit length of the tubing.

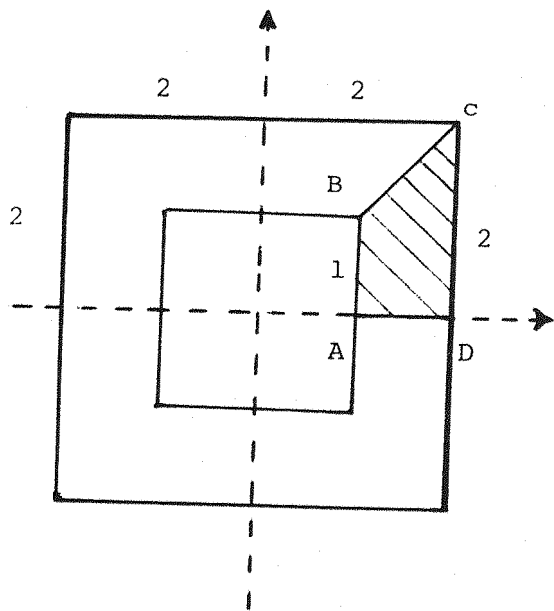


Figure 7 Square Tubing - Cross Section

4.1.1 The upper bound

For finding the upper bound of capacitance, the variation is performed on the volume potential ϕ with the boundary surface potential ϕ_s fixed. The functional to be used is given by equation (3.14),

$$Y = \int_V \frac{1}{2} \epsilon |\underline{E}|^2 dv \quad (4.1)$$

At the minimum of Y , Euler-Lagrange Equation corresponding to that given by equation (2.11) is satisfied by the solution $\phi = \phi_1$. For the square tubing in Figure 1, by symmetry we need only to calculate one eighth of the section denoted by ABCD. See Figure 8. The system equations are given by,

$$\nabla \phi = -\underline{E} \quad (4.2)$$

$$\nabla \cdot \underline{D} = 0 \quad (4.3)$$

while the boundary conditions are,

$$\phi_1(1) = V$$

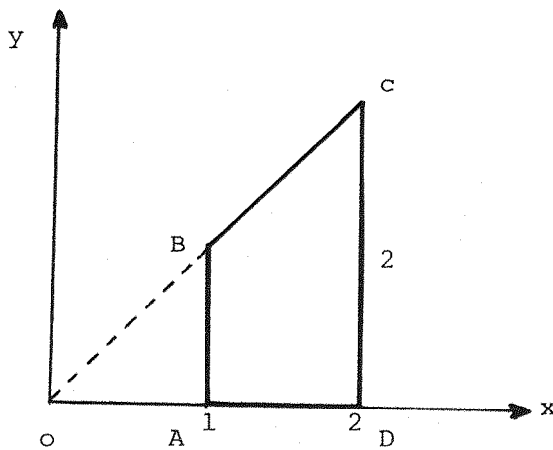
$$\text{and } \phi_1(2) = 0 \quad (4.4)$$

A suitable function of ϕ_1 which satisfies equations (4.3) and (4.4) above is given by,

$$\phi_1 = V(2-x) \quad (4.5)$$

The electric field strength corresponding to this solution of potential is

$$\underline{E}_1 = -\nabla \phi_1 = \underline{Vi} \quad (4.6)$$



$$\phi_1(1) = V \quad \phi_1(2) = 0$$

Figure 8 Capacitance of Tubing Fixed Potential

where \underline{i} is a unit vector in the x -direction.

The system potential energy, from equation (4.1) is given by

$$Y_1 = \int_v \frac{1}{2} \epsilon |\underline{E}_1|^2 dv \quad (4.7)$$

Assuming that ϵ is constant, we have

$$\begin{aligned} Y_1 &= \int_1^2 \int_0^x \frac{1}{2} \epsilon |\underline{E}_1|^2 dy dx \\ &= 0.75 \epsilon V^2 \end{aligned} \quad (4.8)$$

This energy can be expressed in terms of capacitance of the region ABCD and the field potential V as,

$$\frac{1}{2} C_+ V^2 = Y_1 = 0.75 \epsilon V^2 \quad (4.9)$$

The upper bound of the capacitance is therefore given by,

$$c_+ = \frac{2y_1}{v^2} = 1.5\epsilon F \quad (4.10)$$

Since this is only one eighth of the whole tubing section, we have the upper bound capacitance of the square tubing,

$$C_+ = 8 \times 1.5\epsilon = 12.0\epsilon F \text{ per unit length} \quad (4.11)$$

4.1.2 Improvement of upper bound

For the improvement of this bound we can use the improvement formula described in section (3.2). From equation (3.16) we have,

$$\phi_2 = \phi_1 + \alpha\phi_c \quad (4.12)$$

The initial approximation ϕ_1 is given by equation (4.5) above and a suitable choice of ϕ_c satisfying the necessary boundary conditions mentioned in section (3.2) is

$$\phi_c = (1-x)(2-x) \quad (4.13)$$

Hence the electric field strength,

$$\underline{E}_c = -\underline{\nabla}\phi_c = (2x-3) \underline{i} \quad (4.14)$$

This is an example which shows that the volume conditions of equation (3.22)

$$\nabla^2\phi_c = 0 \quad (4.15)$$

as mentioned in section (3.2) need not be a necessary condition in the case of variation of potential and the choice of ϕ_c .

From equation (3.19) the functional Y_2 is given by,

$$\begin{aligned}
 Y_2 &= Y_1 - \frac{\frac{1}{2} \left[\int_v \epsilon \underline{E}_1 \cdot \underline{E}_C dv \right]^2}{\int_v \epsilon |\underline{E}_C|^2 dv} \\
 &= 0.75\epsilon - 0.028\epsilon \\
 &= 0.722\epsilon \tag{4.16}
 \end{aligned}$$

The upper bound capacitance for the whole tubing as before is now improved to the value,

$$C_+ = 11.552\epsilon \text{ F per unit length} \tag{4.17}$$

Other suitable choices of ϕ_C can be made and the upper bound of capacitance similarly calculated. Some of the results are given below.

ϕ_C Chosen	Y_2	Upper Bound Capacitance C_+ (F per unit length)
1. $(1-x)^2 (2-x)$	0.735	11.762ϵ
2. $(1-x) (2-x)^2$	0.729	11.667ϵ
3. $(1-x) (2-x) (1-y)$	0.733	11.722ϵ
4. $(1-x) (2-x) (16-y)$	0.6865	10.984ϵ
5. $(1-x) (2-x) (y)$	0.6875	11.000ϵ
6. $(1-x) (2-x) (y^2)$	0.6776	10.841ϵ

From No. 6 above it can be seen that the upper bound can be improved from 12.0ϵ to as low as 10.841ϵ F per unit length.

4.1.3 The lower bound of capacitance

For the calculation of the lower bound we use the Y-functional given by equation (3.1),

$$Y = \int_v \frac{1}{2\epsilon} |\underline{D}|^2 dv \quad (4.18)$$

In this case we are varying the flux density \underline{D} and keeping the total surface charge constant. As before a solution of the flux density $\underline{D} = \underline{D}_1$ for the system, which minimises the Y-functional above, satisfying the Euler-Lagrange Equation is firstly determined. \underline{D}_1 would have to satisfy the system differential equation given by equation (4.3) and provide a fixed surface charge.

For a suitable \underline{D}_1 such that a known fixed surface charge can be determined, we have to resort to a geometrical approach. Because flux density is a vector quantity, its variation is inherently more difficult to manipulate mathematically when compared to the case of the scalar potential shown in the previous sections. The fixed charge on the boundary has to be determined indirectly through a fixed potential specification.

Let the potential between AB and CD in Figure 9 be V volts. The electric field is given by,

$$\underline{E} = \frac{V}{\ell} \hat{\underline{r}} = V \cos\theta \hat{\underline{r}} \quad (4.19)$$

where $\hat{\underline{r}}$ is a unit vector and ℓ the length as shown in Figure 9.

The average flux density,

$$\underline{D} = \epsilon \underline{E} = \epsilon V \cos\theta \hat{\underline{r}} \quad (4.20)$$

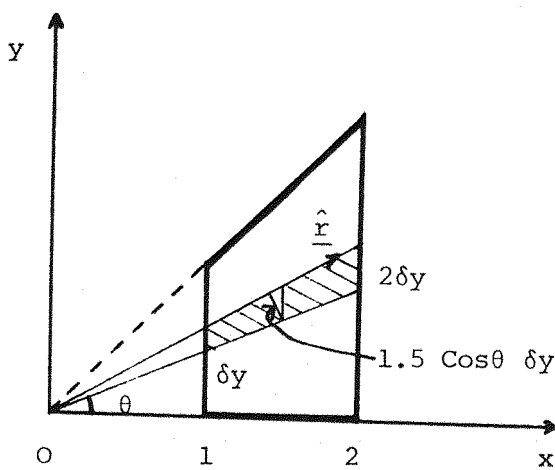


Figure 9 Capacitance of Tubing : Fixed Charge

An incremental charge flowing in a tube of flux is given by

$$\delta Q = |D| \times 1.5 \cos \theta \delta y \quad (4.21)$$

On the surface AB we have the total charge,

$$\begin{aligned}
 Q &= \int_{y=0}^1 1.5\epsilon V \cos^2 \theta \, dy \\
 &= \int_0^{\pi/4} 1.5\epsilon V \cos^2 \theta \sec^2 \theta \, d\theta \\
 &= 1.178\epsilon V C \quad (4.22)
 \end{aligned}$$

The capacitance of the region ABCD is given by,

$$c = \frac{Q}{V} = 1.178\epsilon F \quad (4.23)$$

Therefore the capacitance of the whole square tubing is

$$C = 8c = 9.424\epsilon \quad (4.24)$$

This value, when compared with the upper bound determined in the last section, is a lower bound and the expression of the flux density given by equation (4.20) is a good approximate solution and can be our initial approximation D_1 . The fixed quantity of charge at the surface, \bar{Q} is thus given by equation (4.22).

4.1.4 The improvement of lower bound

For the improvement of the lower bound of inductance we use the expression given by equation (3.3),

$$D_2 = D_1 + \alpha D_C \quad (4.25)$$

A suitable choice of D_C which satisfies the condition stated in equations (3.10) and (3.13) for the boundary and in the volume, is given by

$$\begin{aligned} D_C &= (1-2y) i \quad \text{for } 0 \leq y \leq 1 \\ &= 0 \quad \text{for } y > 1 \end{aligned} \quad (4.26)$$

Using equation (3.7), namely,

$$y_2 = y_1 - \frac{\frac{1}{2} \left[\int_v \frac{1}{\epsilon} D_1 \cdot D_C dv \right]^2}{\int_v \frac{1}{\epsilon} |D_C|^2 dv} \quad (4.27)$$

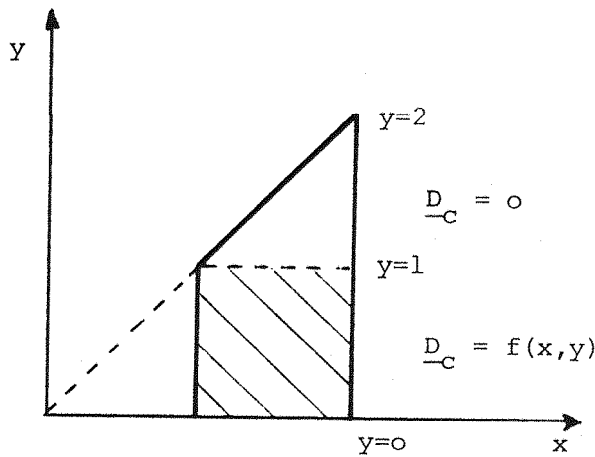


Figure 10 Domain of D_C

we can obtain the value of the improved Y-functional,

$$\begin{aligned}
 Y_2 &= \int_1^2 \int_0^x \frac{1}{2} \epsilon v^2 \cos^2 \theta \, dy \, dx - \frac{\frac{1}{2} \left[\int_0^1 \int_1^2 \frac{1}{\epsilon} \cdot \epsilon v \cos^2 \theta (1-2y) \, dx \, dy \right]^2}{\int_0^1 \int_1^2 \frac{1}{\epsilon} (1-2y)^2 \, dx \, dy} \\
 &= 0.5890 \epsilon v^2 - 0.005 \epsilon v^2 \\
 &= 0.584 \epsilon v^2
 \end{aligned} \tag{4.28}$$

In terms of fixed charges, the capacitive energy is given by

$$Y = \frac{1}{2} \frac{\overline{Q}^2}{C} \tag{4.29}$$

Since Y is a functional with a minimum any variation in its energy gives it a higher energy and hence a lower value than the true capacitance. The lower bound capacitance is thus,

$$C_- = \frac{Q^2}{2Y_2} \quad (4.30)$$

The improved lower bound of capacitance for the region ABCD is given by,

$$\begin{aligned} C_- &= \frac{Q^2}{2Y_2} = \frac{(1.178\epsilon V)^2}{2 \times 0.584\epsilon V^2} \\ &= 1.188\epsilon F \end{aligned} \quad (4.31)$$

The total lower bound capacitance of the square tubing is,

$$C_- = 8C_- = 9.505\epsilon F \text{ per unit length} \quad (4.32)$$

Other choices of \underline{D}_c are possible and results are obtained for the lower bound as below:

<u>\underline{D}_c chosen</u>	<u>Y_2</u>	<u>Lower Bound Capacitance C_-</u> (F per unit length)
1. $(1 - 3y^2) \underline{i}$	0.584ϵ	9.505ϵ
2. $(1 - y - \frac{3}{2y^2}) \underline{i}$	0.584ϵ	9.506ϵ
3. $(1 - \frac{3}{2y} - \frac{3}{4y^2}) \underline{i}$	0.584ϵ	9.505ϵ

It is seen that the calculated lower bound changes very little for the above chosen expressions of D_c . The improvement in the upper bound of capacitance is more substantial compared with the above results. This is as explained before, due to the fact that varying the scalar potential is easier to do than varying the vector flux density as far as the mathematical manipulation is concerned. Furthermore the amount of fixed charges \bar{Q} can only be obtained in an indirect manner because it is the voltage which is specified and thus is itself an estimated value. The use of the Z-functional on the other hand involves terms consisting of the system sources and its improvement as has been mentioned in section 3.3 is difficult compared to that of the Y-functional.

If we take the upper bound capacitance to be $C_+ = 10.841\epsilon$ from the previous sections and the lower bound from this section $C_- = 9.506\epsilon$, we have an average value of capacitance $C = 10.17\epsilon$ as our estimate for the capacitance of the square tubing. The analytical value of the capacitance⁽¹⁾ is 10.25ϵ per unit length. Thus our estimate is less than 1% below the analytical value.

4.2 Calculation of Inductance

To illustrate the calculation of inductance the inverted T-bar conductor, as shown in Figure 11, is used. The dimensions of the bar are shown and J is the current density flowing in the bar.

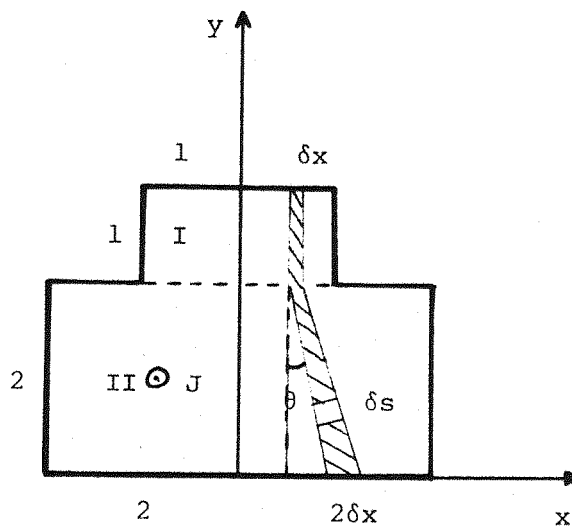


Figure 11 Inverted T-bar Conductor

4.2.1 The upper bound

A geometrical approach is adopted here to calculate the upper bound because a simple algebraic expression to represent the magnetic potentials is difficult to obtain. This should be compared with the calculation of the lower bound of inductance in which simple algebraic expressions can be easily found for the flux density.

The system equations governing this inductive system is given by,

$$\underline{\nabla} \times \underline{H} = \underline{J}$$

$$\underline{\nabla} \cdot \underline{B} = 0$$

$$\underline{B} = \mu_0 \underline{H} \quad (4.33)$$

For the region \mathbb{I} , the Ampere Circuital Law is written for an incremental strip,

$$-(H + \delta H) \delta x + H \delta x = J \delta x \delta y$$

$$\therefore \delta H = -J \delta y \quad (4.34)$$

The average inductance of a small region $\delta x \delta y$ within the incremental strip is given by the relationship,

$$\delta L' = \frac{1}{2} \left(\frac{\delta \Phi}{I} \right) = \frac{-\delta B \delta y}{2J \delta x \delta y} \quad (4.35)$$

For the incremental strip in region \mathbb{I} ,

$$\begin{aligned} \delta L_{\mathbb{I}} &= \int \delta L' \\ &= \int_0^1 \mu_0 J \delta y \\ &= \frac{\mu_0}{2J \delta x} \end{aligned} \quad (4.36)$$

For the whole of region \mathbb{I} and integrating with respect to x , the inductance is given by,

$$\begin{aligned} \frac{1}{L_{\mathbb{I}}} &= \frac{2}{\mu_0} \int_{-1}^1 dx \\ &= \frac{4}{\mu_0} \end{aligned} \quad (4.37)$$

$$\therefore L_I = \frac{\mu_0}{4} \quad (4.38)$$

For the region II, similarly, using the Ampere Circuital Law, we obtain,

$$\delta H = - J \delta s \quad (4.39)$$

The average inductance of a small region given by $1.5 \delta x \cos\theta \delta s$ within an incremental strip is,

$$\begin{aligned} \delta L' &= \frac{1}{2} \left(\frac{\delta \Phi}{I} \right) \\ &= \frac{-\delta B \delta s}{2J (1.5 \delta x \cos\theta) \delta s} \quad (4.40) \end{aligned}$$

The inductance of each incremental strip in region II is

$$\begin{aligned} \delta L_{II} &= \int \delta L' \\ &= \frac{\int_0^{2/\cos\theta} \mu_0 J ds}{3 J \cos\theta \delta x} \\ &= \frac{2\mu_0}{3 \cos^2\theta \delta x} \quad (4.41) \end{aligned}$$

The inductance for the whole of region II is

$$\frac{1}{L_{II}} = \int_{-2}^2 \frac{3 \cos^2\theta dx}{2\mu_0} \quad (4.42)$$

Substituting $dx = 2 \sec^2 \theta dB$, we have

$$\begin{aligned} \frac{1}{L_{II}} &= \int_{\tan^{-1}(-\frac{1}{2})}^{\tan^{-1}(\frac{1}{2})} \frac{3d\theta}{\mu_0} \\ &= \frac{2.782}{\mu_0} \end{aligned} \quad (4.43)$$

$$\therefore L_{II} = 0.3595 \mu_0 \quad (4.44)$$

The total upper bound inductance of the conductor bar is the sum of equations (4.38) and (4.44), thus

$$\begin{aligned} L_+ &= (0.25 + 0.3595) \mu_0 \\ &= 0.6095 \mu_0 \end{aligned} \quad (4.45)$$

The simple improvement formula similar to that given in section 3.2 could not easily be applied to the geometrical approach and hence an improved value for the upper bound could not be obtained. This is, however, not a serious problem and the upper bound obtained can still be used to estimate the bar inductance together with the lower bound value to be obtained in the next section.

4.2.2 The lower bound of inductance

The magnetic flux density B is the field quantity to be varied in the calculation of the lower bound of inductance. Again the inverted T-bar may be divided into two regions as shown in Figure 12.

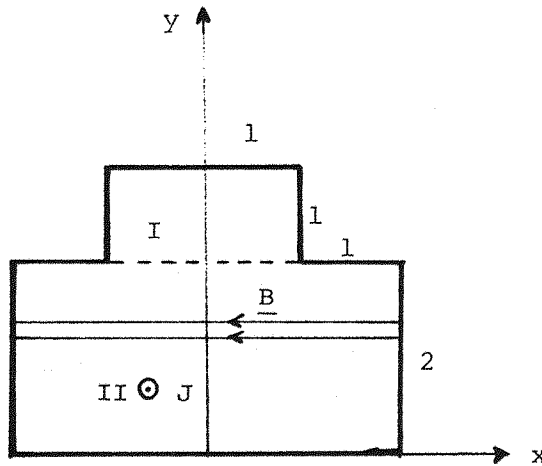


Figure 12 Flux Density in Bar Conductor

Assuming that the flux traverses across the bar in straight horizontal lines, the suitable expressions of \underline{B}_1 satisfying the boundary conditions for both regions are given by,

$$\text{Region I} : \underline{B}_1 = -\mu_0 (2+y) J \underline{i} \quad 2 < y \leq 3$$

$$\text{Region II} : \underline{B}_1 = -\mu_0 y J \underline{i} \quad 0 \leq y < 2 \quad (4.46)$$

The electromagnetic energy is given by,

$$Y_1 = \int_v^3 \frac{1}{2\mu_0} |\underline{B}_1|^2 dv$$

$$\begin{aligned}
 &= \frac{1}{2\mu_0} \int_2^3 \int_{-1}^1 \mu_0^2 J^2 (2+y)^2 dx dy + \frac{1}{2\mu_0} \int_0^2 \int_{-2}^2 \mu_0^2 y^2 J^2 dx dy \\
 &= 25.667 \mu_0 J^2 \quad (4.47)
 \end{aligned}$$

This energy in terms of inductance and source current I is given by,

$$Y_1 = \frac{1}{2} L I^2 \quad (4.48)$$

Using the relationship,

$$L = \frac{\Phi}{I} \quad (4.49)$$

the electromagnetic energy in terms of the flux linkage Φ and the current is given by,

$$Y_1 = \frac{1}{2} \Phi I \quad (4.50)$$

The flux linkage which is the fixed quantity in the variation of the flux density is thus given by,

$$\begin{aligned} \bar{\Phi} &= \frac{2Y_1}{I} \\ &= \frac{2 \times 25.667 \mu_0 J^2}{10J} \\ &= 5.133 \mu_0 J \end{aligned} \quad (4.51)$$

We can now write Y_1 in terms of the flux linkage and the lower bound inductance,

$$Y_1 = \frac{1}{2} \frac{\Phi^2}{L} \quad (4.52)$$

$$\therefore L = \frac{\Phi^2}{2Y_1}$$

$$= \frac{(5.133 \mu_0 J)^2}{2 \times 25.667 \mu_0 J^2}$$

$$= 0.5133 \mu_0 \text{ H per unit length} \quad (4.53)$$

4.2.3 The improvement of lower bound of inductance

The improvement formula obtained in section 3.2 may be used to improve the lower bound inductance. The formula similar to equation (3.7) for this case is,

$$Y_2 = Y_1 - \frac{\frac{1}{2} \left[\int_v \frac{1}{\mu_0} \underline{B}_1 \cdot \underline{B}_C dv \right]^2}{\int_v \frac{1}{\mu_0} |\underline{B}_C|^2 dv} \quad (4.54)$$

Suitable expressions of \underline{B}_C satisfying the boundary and volume conditions of

$$\int \underline{B}_C \cdot d\underline{s} = 0$$

$$\text{and } \nabla \cdot \underline{B}_C = 0 \quad (4.55)$$

are given by,

$$\begin{aligned} \underline{B}_C &= (2 - 2y) \underline{i} & \text{for } 0 \leq y < 2 \\ &= (3y^2 - 10y + 6) \underline{i} & \text{for } 2 < y \leq 3 \end{aligned} \quad (4.56)$$

Taking \underline{B}_1 as given by equation (4.46) and applying equation (4.54), we obtain,

$$\begin{aligned}
 Y_2 &= 25.667 \mu_o J^2 - 0.415 \mu_o J^2 \\
 &= 24.252 \mu_o J^2
 \end{aligned} \tag{4.57}$$

With the fixed flux linkage $\bar{\Phi}$ given by equation (4.51), we obtain the improved value of lower bound using equation (4.52)

$$\begin{aligned}
 L_- &= \frac{\bar{\Phi}^2}{2Y_2} \\
 &= 0.5432 \mu_o H \text{ per unit length}
 \end{aligned} \tag{4.58}$$

Compared with equation (4.53), we see that there is an improvement in the lower bound inductance, not overshooting the value of the upper bound given by equation (4.45).

The average inductance for the conductor bar is calculated from equations (4.45) and (4.58) and we obtain $\frac{1}{2}(0.6095 + 0.5432)\mu_o = 0.5764 \mu_o H$ per unit length. Compared with a numerically⁽²⁾ calculated value of $0.57 \mu_o$, our estimate is within about 1.1% of it.

4.2.4 Difficulties in calculating the upper bound of inductance

While the assumption that magnetic flux traverses horizontally across the bar conductor which is surrounded by highly permeable iron is quite accurate, the situation is different in the case of magnetic potential along the vertical sides of the bar. To assume that the magnetic potential is zero along the sides of the conductor that is surrounded by iron of finite permeability would be inaccurate, as there would always be a small tangential field.

In modelling the bar conductor for the calculation of the upper bound we have in effect 'cut off' the two shaded corners of the bar as shown in Figure 13. This is quite justified as the field at these corners are weak and the energy density would be low. The 'cutting off' also pushes up the value of the bar inductance and we are quite certain to be on the upper bound of the true value. There is still a slight inaccuracy in the modelling of magnetic equipotential lines along the bottom of the conductor as it could not be zero all along it. Again because of the weak fields at the bottom region, this slight inaccuracy does not contribute much to the overall energy of the bar.

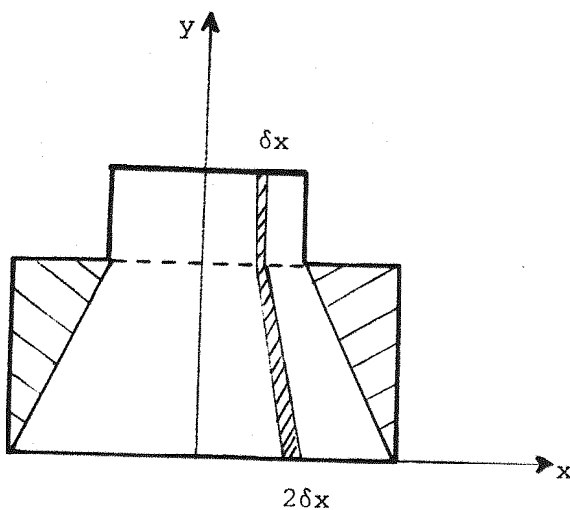


Figure 13 Effective Shape of Bar Conductor

Another possible approximation would be to assume the bar conductor to have an effective shape as shown in Figure 14 in which we have neglected the shaded sections. To maintain the same magnetic field strength in the unshaded region we assume a current density of $2J$ to be flowing in region II instead of just J .

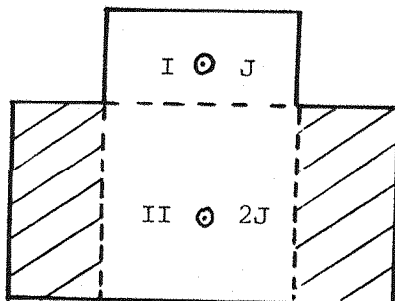


Figure 14 Possible Approximation of Bar Conductor

For this effective shape we can use the magnetic field \underline{H} and express it in an algebraic form, to calculate the magnetic energy. Suitable expressions for \underline{H} would be given by,

$$\begin{aligned}\underline{H} &= -(4+y)J \underline{i} \text{ in region I} \\ &= -2yJ \underline{i} \quad \text{in region II}\end{aligned}\tag{4.59}$$

The electromagnetic energy is given by,

$$\begin{aligned}Y &= \int_V \frac{1}{2} \mu_0 |\underline{H}|^2 dv \\ &= \frac{1}{2} \mu_0 \int_{-1}^1 \int_0^1 (4+y)^2 J^2 dx dy + \frac{1}{2} \mu_0 \int_{-2}^2 \int_0^2 4y^2 J^2 dx dy \\ &= 31.0 \mu_0 J^2\end{aligned}\tag{4.60}$$

The upper bound of inductance by using equation (4.48) is,

$$\begin{aligned}L_+ &= \frac{2Y}{I^2} \\ &= 0.620 \mu_0 \text{ H per unit length}\end{aligned}\tag{4.61}$$

remembering that $I = 10J$.

The upper bound we obtain in section 4.2.1 is $0.6095 \mu_0 \text{ H}$. If the upper bound of equation (4.61) is used, we have an average inductance of $\frac{1}{2} \mu_0 (0.5432 + 0.620) = 0.5816 \mu_0 \text{ H}$ per unit length which is only about 2% above the value $0.57 \mu_0 \text{ H}$. It is thus quite possible that a suitable approximation can be used in the calculation of the upper bound to overcome the difficulty in obtaining simple algebraic expressions for the original problem.

4.3 Calculation of Resistance

The calculation of the resistance of a square plate of dimension as shown in Figure 15 is considered. The plate has a thickness b and conductivity σ . The equations governing this resistive system is given by,

$$-\underline{\nabla}\phi = -\underline{E}$$

$$\underline{\nabla} \cdot \underline{J} = 0$$

$$\underline{J} = \sigma \underline{E}$$

(4.62)

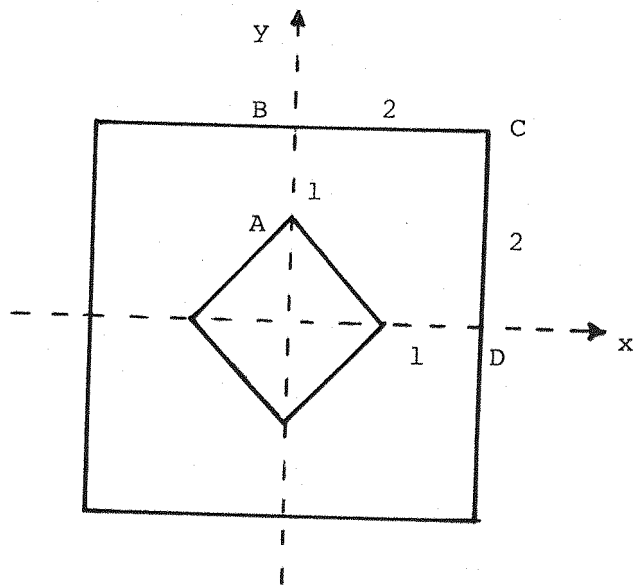


Figure 15 Resistive Plate

4.3.1 The upper bound

In the calculation of the upper bound the current I is the fixed quantity and the variation is performed on the current density \underline{J} . A suitable current density \underline{J}_1 such that it is the solution of the Euler-Lagrange Equation has to be determined first.

Consider a quarter of the plate given by the sides ABCD as shown in Figure 13. Let the potential difference between the sides AB and CD be V volts.

The electric field strength is then given by,

$$\underline{E} = \frac{V}{l} \hat{\underline{r}} \quad (4.63)$$

where $\hat{\underline{r}}$ is the unit vector and l the length as shown in Figure 16.

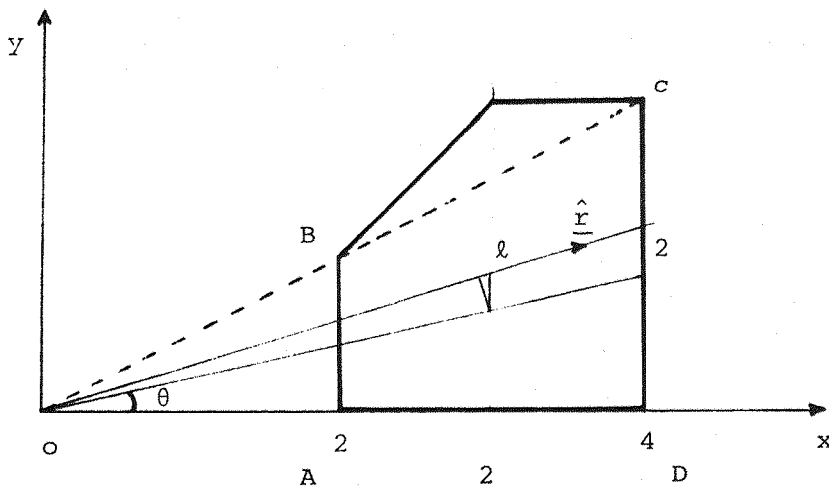


Figure 16 Modelling the Current Flow

Substituting for $\ell = 2/\cos\theta$ into the above equation we obtain,

$$\underline{E} = \frac{V \cos\theta}{2} \hat{\underline{r}} \quad (4.64)$$

The average current density is thus given by,

$$\underline{J} = \sigma \underline{E}$$

$$= \frac{\sigma V \cos\theta}{2} \hat{\underline{r}} \quad (4.65)$$

This expression of current density can be taken as our initial approximate solution \underline{J}_1 .

The average incremental current is,

$$\delta I = b |\underline{J}_1| \times 1.5 \delta y \cos\theta \quad (4.66)$$

Thus the total current flowing from AB to CD is given by,

$$\begin{aligned} I &= \int \delta I \\ &= b \int_{y=0}^1 |\underline{J}_1| \cdot 1.5 \cos\theta dy \quad (4.67) \end{aligned}$$

Substituting for \underline{J}_1 and $dy = 2 \sec^2\theta d\theta$,

$$\begin{aligned} I &= \frac{\sigma b}{2} \int_0^{\tan^{-1}(\frac{1}{2})} 1.5 V \cos^2\theta \cdot 2 \sec^2\theta d\theta \\ &= 0.6955 V \sigma b \quad (4.68) \end{aligned}$$

The upper bound resistance of the plate is given by,

$$R_+ = \frac{V}{I} = 1.4378/\sigma b \Omega \quad (4.69)$$

It is noted that the above modelling cuts off the shaded corner of the plate shown in Figure 17. This pushes the resistance slightly higher than the value that would have been obtained when there is no such 'cutting off'.

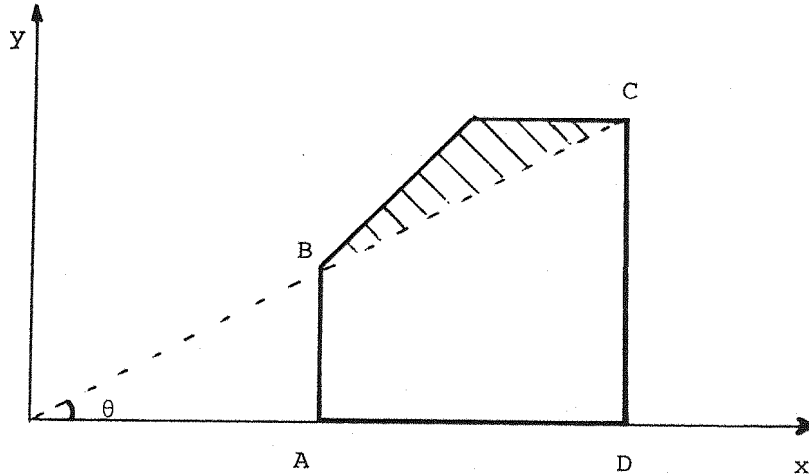


Figure 17 Effective Shape of Resistive Plate

4.3.2 The improvement of the upper bound resistance

The value of the upper bound of resistance given in equation (4.69) above can be improved by using the improvement scheme shown in section 3.2. The corresponding formula similar to equation (3.7) for this case is,

$$Y_2 = Y_1 - \frac{\frac{b}{2} \left[\int_v \frac{1}{\sigma} \underline{J}_1 \cdot \underline{J}_c dv \right]^2}{\int_v \frac{1}{\sigma} |\underline{J}_c|^2 dv} \quad (4.70)$$

where \underline{J}_1 is given by equation (4.65) and Y_1 is

$$Y_1 = \frac{b}{2} \int_v |\underline{J}_1|^2 dv \quad (4.71)$$

The conditions which \underline{J}_c must satisfy for the above improvement formula to be applicable are similar to those given in equations (3.10) and (3.13), namely the boundary conditions,

$$\int_s \underline{J}_c \cdot \underline{ds} = 0 \text{ at sides AB and CD} \quad (4.72)$$

and the volume conditions,

$$\nabla \cdot \underline{J}_c = 0 \quad (4.73)$$

A possible choice is given by,

$$\begin{aligned} \underline{J}_c &= (1-2y) \underline{i} \quad \text{for } 0 < y \leq 1 \\ &= 0 \quad \text{for } y > 1 \end{aligned} \quad (4.74)$$

For this choice of \underline{J}_c , equation (4.70) yields,

$$\begin{aligned} y_2 &= 0.3477 v^2 \sigma b - 0.00026 v^2 \sigma b \\ &= 0.3474 v^2 \sigma b \end{aligned} \quad (4.75)$$

In terms of the upper bound resistance and the fixed current I ,

$$y_2 = \frac{1}{2} I^2 R_+ \quad (4.76)$$

Using equations (4.68) and (4.75), we can determine the upper bound resistance, improved,

$$R_+ = \frac{2y_2}{I^2} = 1.4364/\sigma b \Omega \quad (4.77)$$

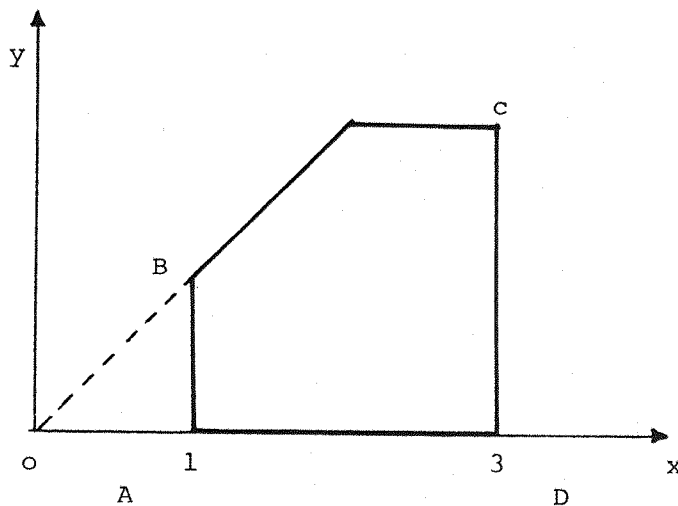
It is seen that there is only a very slight improvement by bringing the upper bound resistance from $R_+ = 1.4378/\sigma b$ down to $R_+ = 1.4364/\sigma b$.

Other suitable expressions of \underline{J}_c may be chosen and some examples are given below:

\underline{J}_c chosen	y_2	Upper Bound Resistance $R_+/\sigma b \Omega$
1. $(1-y - \frac{3}{2} y^2) \underline{i}$	0.3475	1.4366
2. $(1-3y^2) \underline{i}$	0.3475	1.4366
3. $(2y-3y^2) \underline{i}$	0.3475	1.4368
4. $(3y^2-4y^3) \underline{i}$	0.3476	1.4371

4.3.3 The lower bound of resistance

The calculation of the lower bound involves the variations of the potential ϕ in the volume with the boundary potentials at AB and CD fixed, as shown in Figure 18.



$$\phi_1(1) = V \quad \phi_1(3) = 0$$

Figure 18 Fixed Potential on Resistive Plate

An approximation solution ϕ_1 of the potential which satisfies the Euler-Lagrange Equation and the boundary conditions of fixed potential is first determined. The potential ϕ_1 also satisfies the system equations which are given by,

$$\nabla^2 \phi_1 = 0 \quad (4.78)$$

$$\underline{\nabla} \phi_1 = -\underline{E}_1$$

A suitable expression of ϕ_1 which satisfies the above equation is

$$\phi_1 = \frac{1}{2} V (3-x) \quad (4.79)$$

The resistive system energy is then given by,

$$\begin{aligned} Y_1 &= \int_v^2 \frac{\sigma b}{2} |\underline{E}_1|^2 dv \\ &= \int_1^2 \int_0^x \frac{\sigma b}{2} |\underline{E}_1|^2 dx dy + \int_2^3 \int_0^2 \frac{\sigma b}{2} |\underline{E}_1|^2 dx dy \\ &= 0.4375 \sigma b V^2 \end{aligned} \quad (4.80)$$

In terms of the lower bound resistance and the fixed potential V , the energy Y_1 can be written as,

$$Y_1 = \frac{1}{2} \frac{V^2}{R_-} \quad (4.81)$$

And from equation (4.80) above, the lower bound resistance is,

$$R_- = \frac{V^2}{2Y_1} = 1.143/\sigma b \Omega \quad (4.82)$$

4.3.4 The improvement of lower bound of resistance

For the improvement of the lower bound value the improvement formula given by (3.7) in section 3.2 may be used. For this case corresponding to equation (3.7), we have the improved system energy Y_2 given by,

$$Y_2 = Y_1 - \frac{\frac{b}{2} \left[\int_v \sigma \underline{E}_1 \cdot \underline{E}_C dv \right]^2}{\int_v \sigma |\underline{E}_C|^2 dv} \quad (4.83)$$

where \underline{E}_C is given by,

$$\underline{E}_C = -\nabla \phi_C \quad (4.84)$$

and ϕ_C is such that it satisfies the boundary conditions mentioned in section 3.2, namely,

$$\phi_C(1) = \phi_C(3) = 0 \quad (4.85)$$

The volume condition of $\nabla^2 \phi_C = 0$ as mentioned in section 3.2 is not a necessary condition in the choice of ϕ_C .

A possible choice of ϕ_C satisfying the boundary conditions is,

$$\phi_C = V(1-x)(3-x) \quad (4.86)$$

The electric field is then,

$$\underline{E}_C = -\nabla \phi_C = V(2x-4) \underline{i} \quad (4.87)$$

The improved system energy from equation (4.83) is given by,

$$\begin{aligned} Y_2 &= 0.4375 \sigma b v^2 - 0.0128 \sigma b v^2 \\ &= 0.4247 \sigma b v^2 \end{aligned} \quad (4.88)$$

The improved lower bound resistance by equation (4.82) is,

$$\begin{aligned} R_- &= \frac{v^2}{2Y_2} \\ &= 1.177/\sigma b \Omega \end{aligned} \quad (4.89)$$

Other possible choices of ϕ_c can be made. Similar calculation is made and the results are given below.

<u>ϕ_c chosen</u>	<u>$Y_2 \sigma b V^2$</u>	<u>Lower Bound Resistance $R_-/\sigma b \Omega$</u>
1. $(1-x)^2 (3-x)^2$	0.4348	1.1499
2. $(1-x)^2 (3-x)^2$	0.4291	1.1654
3. $(1-x) (3-x) (1-y)$	0.4310	1.1601
4. $(1-x) (3-x) (y)$	0.4148	1.2055
5. $(1-x) (3-x) (y^2)$	0.4160	1.2019

If the best of the lower bounds, that is $R_- = 1.2055/\sigma b \Omega$ and the best of the upper bounds from section 4.3.2, that is $R_+ = 1.4366/\sigma b \Omega$ are taken to estimate the plate resistance, we obtain an average value of $1.321/\sigma b \Omega$. Compared with the solution obtained by a finite difference method⁽³⁾ which gives $R = 1.34/\sigma b \Omega$, our estimate is within 1.5% of it.

4.4 The Calculation of Resistance and Reactance of Time-Varying Electromagnetic Systems

A full calculation of the resistance and reactance of time varying electromagnetic systems has not been undertaken. Calculations were made to check the results obtained in reference (4) in which a full account is given.

The problem considered is that of a thick conducting slab of conductivity σ and skin depth δ as shown in Figure 19.

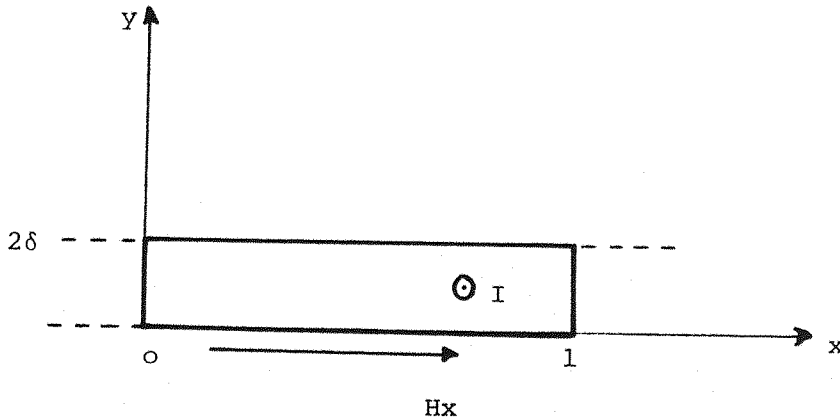


Figure 19 Thick Conducting Slab

By using the Y-functional mentioned in section 2.7,

$$Y = \int_V \frac{1}{2\sigma} (\underline{J} \cdot \underline{J}^*) + \frac{j\omega\mu}{2} (\underline{H} \cdot \underline{H}^*) dv \quad (4.90)$$

and the variational statement,

$$\delta Y = \mu\omega \int_V (\underline{H}'' \cdot \delta \underline{H}'') - (\underline{H}' \cdot \delta \underline{H}'') - \frac{j}{\sigma} (\underline{J}'' \cdot \delta \underline{J}') + \frac{j}{\sigma} (\underline{J}' \cdot \delta \underline{J}'') = 0 \quad (4.91)$$

where

$$\underline{J} = J' + jJ''$$

$$\underline{J}^* = J' - jJ''$$

$$\underline{H} = H' + jH''$$

$$\underline{H}^* = H' - jH'' \quad (4.92)$$

the lower bound resistance and the upper bound reactance can be calculated, where

$$(R_- + jX_+) = \int_v \frac{1}{2\sigma} (\underline{J} \cdot \underline{J}^*) + \frac{j\omega\mu}{2} (\underline{H} \cdot \underline{H}^*) dv \quad (4.93)$$

The trial function,

$$\underline{H} = \frac{I}{2} + \alpha_1 y + \alpha_2 y^2 + j(\beta_1 y + \beta_2 y^2) \quad (4.94)$$

is used and the results obtained were, $R_- = 0.4532/\sigma\delta \Omega$ and $X_+ = 0.5040/\sigma\delta \Omega$.

When the trial function,

$$\underline{H} = \frac{I}{2} + \alpha_1 y + \alpha_2 y^2 + \alpha_3 y^3 + j(\beta_1 y + \beta_2 y^2 + \beta_3 y^3) \quad (4.95)$$

was used, we obtain $R_- = 0.4763/\sigma\delta \Omega$ and $X_+ = 0.5000/\sigma\delta \Omega$.

Further when the trial function,

$$\underline{H} = \frac{I}{2} + \alpha_1 y + \alpha_2 y^2 + \alpha_3 y^3 + \alpha_4 y^4 + j(\beta_1 y + \beta_2 y^2 + \beta_3 y^3 + \beta_4 y^4)$$

(4.96)

was used, the results were $R_- = 0.4632/\sigma\delta \Omega$ and $X_+ = 0.5029/\sigma\delta \Omega$.

The analytical results are $R = 0.5\Omega$ and $X = 0.5\Omega$. It can be seen that there is an improvement in the values of R_- and X_+ when equation (4.95) is used as the trial function, instead of equation (4.94). The same improvement would have been expected in using equation (4.96) instead of equation (4.95) as the trial function. This is, however, not the case. The matter was not pursued further due to lack of time.

The computer program used to calculate the last two cases of trial functions is given in Appendix III.

References

1. HAMMOND, P. : 'Energy Methods in Electromagnetism', Clarendon Press, Oxford (1981), p 129.
2. As above, p 130.
3. As above, p 124.
4. HAMMOND, P. and PENMAN, J. : 'Calculation of Eddy Currents by Dual Energy Methods', Proc. IEE, Vol. 125 (7), July 1978, pp 701-708.

CHAPTER FIVE

THE APPLICATION OF THE FIELD VARIATIONAL METHOD TO MACHINE DESIGN

The field variational method is shown in this chapter to be applied to the calculation of stator slot leakage reactance of an induction motor. It also shows a means of achieving a better estimate of the slot leakage reactance of a winding at the bottom of a very deep slot.

5.1 The Slot Description

The unusually deep slot which belongs to a 2-speed, 3.8 kV, 3 phase, 50 Hz, 2.2 kW induction motor is shown in Figure 20. The slot has a magnetic wedge. The high speed winding (10-pole) with 6 conductors and pitched at 0.75 p.u. is at the bottom of the slot with the low-speed (14-pole) at the top; both being insulated from the iron. Based on the standard calculation methods of Alger⁽¹⁾, Liwschitz⁽²⁾ and Richter⁽³⁾ the calculated total leakage reactance of this motor for the high-speed (10-pole) winding is 4.44Ω of which 2.68Ω is the stator slot leakage reactance. Thus the stator slot leakage represents about 60% of the total leakage reactance. Surprisingly however, the test results obtained by the machine manufacturer was 5.25Ω . The calculated value is therefore about 15.2% below the test value. On the other hand the total motor leakage reactance of the low-speed (14-pole) winding calculated by the standard methods was 9.72Ω , about 6.6% below the test value of 10.41Ω .

5.2 Calculation of the Lower Bound of Slot Reactance due to the Lower Winding

The calculation of the lower bound of reactance is similar to the lower bound inductance calculation shown in section 4.2. The actual slot shape of the machine is as shown in Figure 20 but for the purpose of our calculation a simplified shape as shown in Figure 21 is taken. The tooth-neck of $h_3 = 0.105"$ is an approximation obtained by adding 0.04" to $\frac{1}{2}(0.170" - 0.04")$. The effect of possible tooth-tip saturation is neglected and the values of reactance mentioned are all unsaturated values.

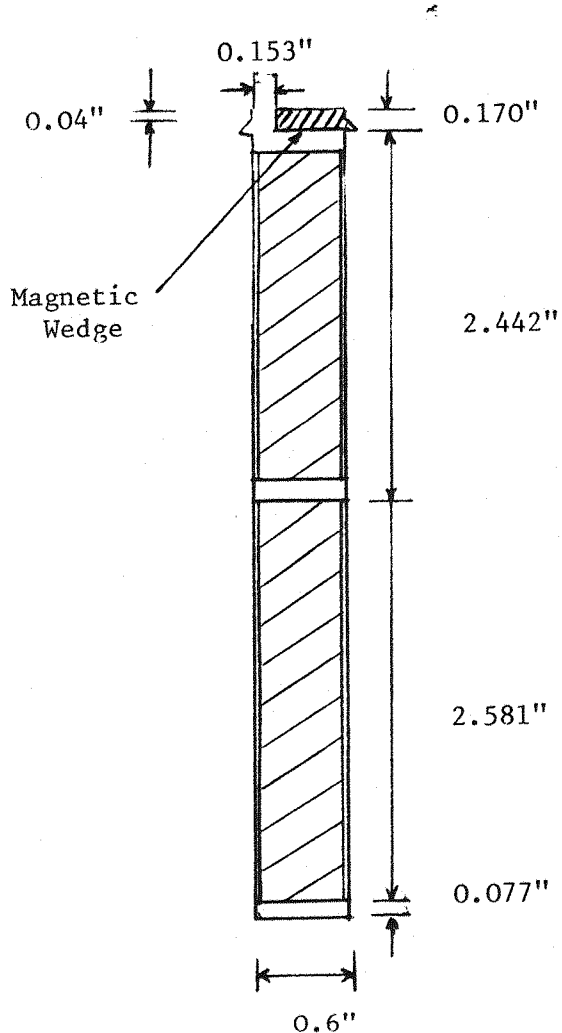


Figure 20 Actual Stator Slot Shape

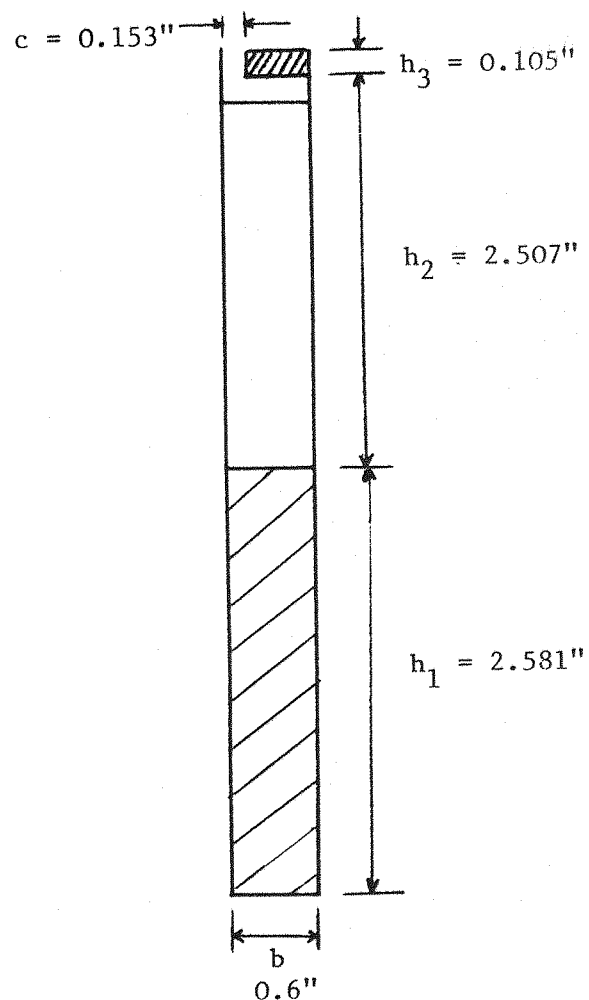


Figure 21 Simplified Slot Shape

Normal design office methods use an approximate flux plot for the calculation of reactance. It is shown in reference (4) that all such methods give a lower bound to the inductance. In physical terms the flux seeks the easiest route and any approximation introduces constraints which reduce the permeance and hence the inductance and the reactance.

As mentioned in section 2.3 in the approach using the 2-Y functionals the field quantity used in the calculation of the lower bound of inductance is the magnetic flux density \underline{B} and the imposed source being the total flux linkages $N\Phi$. The Y-functional in terms of \underline{B} is given by equation (2.34),

$$Y = \int_v \frac{1}{2\mu_0} |\underline{B}|^2 dv \quad (5.1)$$

where the integration is done over the defined region. For the stator slot per unit length, the defined region is given by the slot opening and the surrounding highly permeable iron. We can use μ_0 for the permeability because the iron is excluded from the defined region.

The Y-functional as stated in section 2.3 is a convex energy functional having a minimum of energy. Any variation in the field \underline{B} would give an increase in the energy Y which is higher than its minimum. In terms of the fixed sources $N\Phi$ and the inductance L, the Y-functional may be written as,

$$Y = \frac{1}{2} \frac{(N\Phi)^2}{L} \quad (5.2)$$

Thus the inductance is given by,

$$L = \frac{(N\Phi)^2}{2Y} \quad (5.3)$$

Physically as has been mentioned in section 3.4 the variation in the magnetic flux density B can be achieved by the conceptual insertion of magnetic flux barriers of negligible thickness. These flux barriers shape the magnetic flux flow tubes. This shaping causes an increase in the potential energy Y of the system. With the flux linkages remaining constant, we can see from equation (5.3) that an increase in Y means a decrease in the inductance L and hence we have a lower bound inductance. Alternatively as mentioned earlier it can also be seen as putting constraints upon the flux flow due to the introduction of flux barriers, causing a reduction in the permeance and hence a decrease in the inductance from its true value. The calculation of inductance using a flux plot therefore always provides a lower bound of inductance.

It is a well-known design fact that a good approximation for B in a slot surrounded by iron of high permeability is given by parallel lines across the slot perpendicular to the slot sides. This approximation does not require infinite permeability as is sometimes thought. All that is required is that the flux should enter the iron nearly at right angles which is likely even where the permeability is of the order of 100. Such an approximation for B therefore represents a sound basis in design calculations. For our calculation of the lower bound the same assumption has been adopted. The approximate expression of flux density obtained would correspond to B_1 , the approximate solution which satisfies the Euler-Lagrange Equation mentioned in section 2.2 such that the Y -functional of equation (5.1) above is a minimum.

The slot shown in Figure 21 may be divided into three regions, namely that denoted by h_1 for the current-carrying part, and h_2 , h_3 for those above the conducting region. The number of turns or conductors in the slot is denoted by N and the current flowing in each conductor I .

By using the Ampere Circuital Law,

$$\oint H \, dl = mmf \quad (5.4)$$

we can write down for each of the region the following,

$$\text{Region } h_1 : H \times b = - \left(\frac{y}{h_1} \right) NI \rightarrow B = -\mu_0 \frac{NI}{bh_1} y$$

$$h_2 : H \times b = -NI \rightarrow B = -\mu_0 \frac{NI}{b}$$

$$h_3 : H \times c = -NI \rightarrow B = -\mu_0 \frac{NI}{c} \quad (5.5)$$

where y is the space variable of the stator slot height. For details of the calculation see Appendix IV.

By substituting equation (5.5) into equation (5.1) and summing over the three regions we obtain,

$$y = \mu_0 N^2 I^2 \left[\frac{h_1}{6b} + \frac{h_2}{2b} + \frac{h_3}{2c} \right] \quad (5.6)$$

In terms of the current I and the inductance, the Y -functional can be written as,

$$Y = \frac{1}{2} LI^2 \quad (5.7)$$

From equations (5.6) and (5.7) we have the expression of the inductance,

$$L = \frac{2Y}{I^2} = \mu_0 N^2 \left[\frac{h_1}{3b} + \frac{h_2}{b} + \frac{h_3}{c} \right] \quad (5.8)$$

Because of the assumptions made, the inductance given by equation (5.8) above is the lower bound value. This is also the standard result obtained in textbooks; see reference (5) for example, except that it does not seem widely known that it provides a lower bound for the correct solution.

Using the relationship,

$$L = \frac{N\Phi}{I} \quad (5.9)$$

we can write down the flux linkage as,

$$N\Phi = LI \quad (5.10)$$

Therefore the fixed flux linkages from equation (5.8) is given by,

$$N\Phi = \mu_0 N^2 I \left[\frac{h_1}{3b} + \frac{h_2}{b} + \frac{h_3}{c} \right] \quad (5.11)$$

Evaluation of equation (5.8) using the dimensions shown in Figure 21 with $N = 6$, gives the lower bound inductance,

$$L = 226.703 \mu_0 \text{ H per unit length} \quad (5.12)$$

The length of the slot is 34.5" and there are 40 slots per phase. The total slot reactance per phase is thus,

$$X_s = 3.137 \Omega \text{ per unit length} \quad (5.13)$$

5.3 The Improvement of the Lower Bound of Inductance

As indicated in equation (5.1), the Υ -functional is a quadratic functional in the flux density \underline{B} and has a minimum of energy as shown in Figure 22.

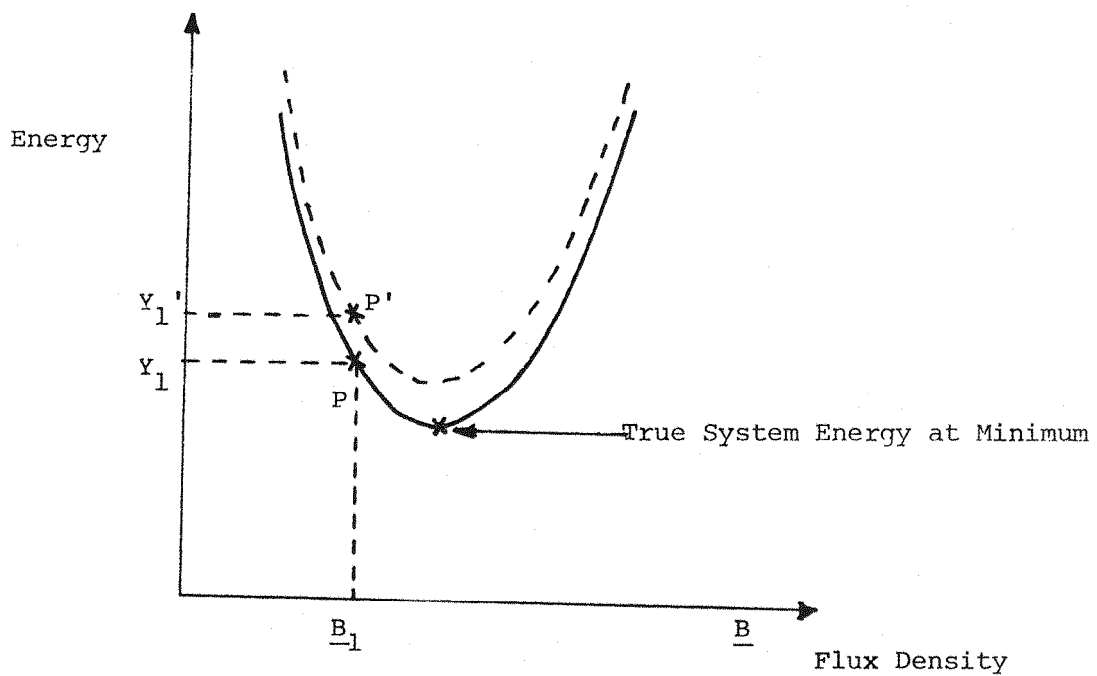


Figure 22 Approximate System Energy Functional

A good approximation of \underline{B}_1 of the flux density as shown in section 5.2 would place us at a point P of the functional. This approximate \underline{B}_1 would necessarily need to satisfy the boundary conditions of the slot as well as the volume condition in terms of the imposed sources so that point P is on the energy functional describing the system. In practice the choice of \underline{B}_1 in the calculation of the lower bound of inductance as explained earlier is not difficult. The boundary conditions can be easily and quite accurately met and the volume conditions merely require that \underline{B}_1 is solenoidal in the slot. In cases where the volume and boundary conditions for \underline{B}_1 is not exactly satisfied, the energy due to \underline{B}_1 may be at point P' shown in Figure 22. We are in this case on an energy functional which is slightly displaced from the true one. This would not pose a problem to the bound we obtain as any approximation in \underline{B}_1 using approximate boundary and volume conditions will always give a calculated energy which is higher than the true system energy. The true system energy is always the minimum value of the system energy. This will be the case in the calculation of the upper bound in section 5.4 when we modify the boundary conditions to obtain an effective slot shape.

Improvement on the lower bound inductance given by equation (5.8) can be achieved by using the improvement formula given in section 3.2. Corresponding to equation (3.3) we have,

$$\underline{B}_2 = \underline{B}_1 + \alpha \underline{B}_C \quad (5.14)$$

where \underline{B}_C needs to satisfy the boundary conditions that the total flux due to it is zero. Thus,

$$\int \underline{B}_C \cdot d\underline{s} = 0 \quad (5.15)$$

The flux density \underline{B}_C has to be solenoidal in the volume, thus

$$\nabla \cdot \underline{B}_C = 0 \quad (5.16)$$

For the slot per unit length as in Figure 21 equations (5.15) and (5.16) become simply,

$$\int B_C dy = 0 \quad (5.17)$$

and $\frac{\partial}{\partial x} B_C = 0$

for each of the three regions of the slot.

The expressions of \underline{B}_1 for each of the three regions of the slot is given by equation (5.5). The electromagnetic energy Y_2 due to \underline{B}_2 corresponding to equation (3.7) is given by,

$$Y_2 = Y_1 - \frac{\frac{1}{2} \left[\int_V \frac{1}{\mu_0} \underline{B}_1 \cdot \underline{B}_C dv \right]^2}{\int_V \frac{1}{\mu_0} |\underline{B}_C|^2 dv} \quad (5.18)$$

Equation (5.18) is applied to each of the three regions of the slot. We notice that for the two regions above the current-conducting region where \underline{B}_1 is independent of the space variable y , the second term on the

right hand side of equation (5.18) becomes identically zero due to the requirement that \underline{B}_c has to satisfy equation (5.17). There is no change in the value of Y_1 . This is because in the non-conducting regions we have assumed a constant flux density which is known everywhere and thus is not affected by any field variation introduced.

For the current-carrying region a possible choice of \underline{B}_c satisfying the conditions of equation (5.17) is,

$$\underline{B}_c = (y - 1.291) \underline{i} \quad (5.19)$$

where \underline{i} denotes the unit vector in the x-direction. For details of calculation see Appendix V.

By substituting \underline{B}_1 from equation (5.5) and \underline{B}_c from equation (5.19) into equation (5.18) we obtain the value of Y_2 for each of the slot regions.

From equation (5.3) for fixed flux linkages $N\Phi$ and a reduction in the system energy from Y_1 to Y_2 , we obtain an improvement of the lower bound inductance. By putting the value of Y_2 obtained into equation (5.3) we obtain the improved lower bound value of inductance,

$$L_ = 231.435 \mu_o \text{ H per unit length} \quad (5.20)$$

As in equation (5.13) we obtain the reactance per phase as

$$X_s = 3.203 \Omega \text{ per unit length} \quad (5.21)$$

which is an increase of about 2% over the value given by equation (5.13). This is not a very substantial improvement. It was found as in section 4.1.4 for the lower bound improvement of capacitance using \underline{D}_c , that other choices of \underline{B}_c , for example using higher order expressions in y , gave no appreciable improvement as well.

The difficulty in improving besides the fact that we are dealing with a vector quantity, can be further attributed to the fact that the fixed flux linkages $N\Phi$ is an approximation itself because it is the current which is specified. It is difficult to specify the total flux linkages whereas to specify the current would be comparatively easy. An accurate $N\Phi$ is required for the improvement of the lower bound to be substantial. This is similarly the case in the calculation of capacitance, inductance and resistance in Chapter 4. In cases of fixed potential we have a substantial improvement whereas in cases of fixed charges or fixed flux linkages we only have a small improvement.

We can consider the upper bound to the inductance as a means of achieving a better estimate of the true inductance.

5.4 Determination of the Upper Bound of Inductance due to the Lower Winding

In calculating the upper bound of inductance as mentioned in section 4.2, the magnetic potential along which the magnetic field H is zero is the quantity to be varied. The fixed sources being the current I , flowing in each conductor. Figure 23 shows the slot with the equipotential lines. The effective slot shape is as shown for the following reasons. Whereas in the case of the lower bound calculation, the assumption of normal flux density at the slot side is an acceptable one without resorting to the use of an effective slot shape this is not the case here. We have a more stringent requirement for the variation in magnetic potential in that the tangential field should be zero along the slot side; it being an equipotential surface. This would imply an extremely high value of permeability for the surrounding iron. Clearly there is a circulation of flux at the bottom of the slot due chiefly to the position of the lower

winding being surrounded on three sides by iron of finite permeability. The current-carrying region has therefore to be modified to an effective shape to take such effects into account, such that we have a condition which is closer to that of the actual machine slot. The effective slot shape has only one point at which the potential is zero instead of the whole slot bottom as when we assume infinite permeability of iron. Such a point is known as a kernel and is at the centre of the slot bottom. That there is one such kernel for such a slot has previously been shown by Stevenson and Park⁽⁶⁾.

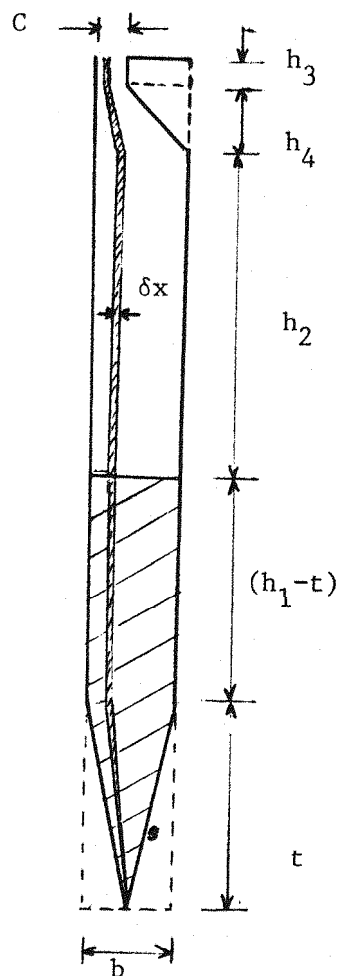


Figure 23 Effective Slot Shape

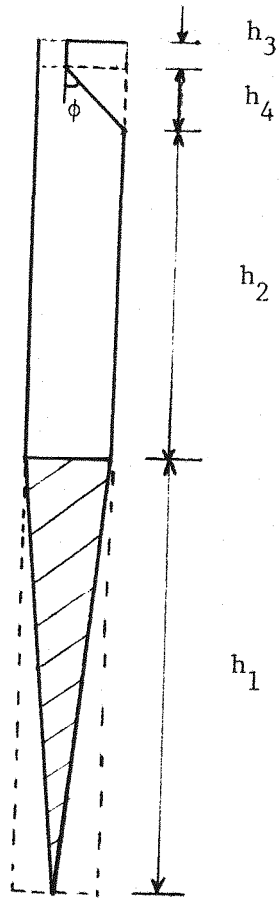


Figure 24 Alternative Effective Slot Shape

Alternatively, the effective slot shape shown in Figure 24 may be used. In this case we are allowing for the effects of flux circulation due to the lower winding to extend higher into the upper part of the current-carrying region.

In calculating the upper bound of inductance, the Y-functional is expressed in terms of the fixed current source I , thus,

$$Y = \frac{1}{2} LI^2 \quad (5.22)$$

The variation is performed on the magnetic potential or the lines of no work if within the current-carrying region. As mentioned in section 3.4 for the case of electric potential, the variation in the magnetic potential can be performed by the conceptual insertion of infinitely permeable sheets of negligible thickness. The equipotential lines are shaped by these sheets and such shaping increases the system potential energy. From equation (5.22) we can see that any increase in Y from its minimum with I fixed means an increase in the inductance from its true value; hence the upper bound of inductance.

Simple algebraic expressions for such equipotential lines are difficult to find. A geometrical approach can usefully be adopted for the calculation of the upper bound and is shown below.

The slot is divided into five regions as shown in Figure 23. The inductance of each region is calculated by summing up the inductance due to each incremental strip between two equipotential lines. The expression of \underline{H} for each region is given by,

$$\text{Region } t : \delta H = - \frac{Nj}{h_1} s \cos\theta \delta s$$

$$(h_1 - t) : \delta H = - \frac{Nj}{h_1} y \delta y$$

$$h_2 : H = - \frac{NI}{b}$$

$$h_3 : H = - \frac{NI}{c}$$

$$h_4 : H = - \frac{-2NI}{(b+c)\cos\theta} \quad (5.23)$$

where N = no. of conductors in the lower winding of the slot,

J = the average current density, I = the current flowing in each conductor. For details of calculation see Appendix VI.

From the above expressions it is seen that the magnetic field for the current carrying regions is expressed as an increment δH whereas for the non-conducting region where the magnetic field is constant, simply H . The relationship of equation (5.9),

$$L = \frac{N\Phi}{I} \quad (5.24)$$

is used to calculate the inductance of each incremental strip and the inductance of each region is obtained separately by integration.

We obtain the following expressions of inductance for the upper bound,

$$\text{Region } t : L = \frac{\mu_0 N^2 t^2}{3h_1^2 \tan^{-1} (b/2t)}$$

$$(h_1 - t) : L = \frac{\mu_0 N^2 (h_1^3 - t^3)}{3h_1^2 b}$$

$$h_2 : L = \frac{\mu_0 N^2 h_2}{b}$$

$$h_3 : L = \frac{\mu_0 N^2 h_3}{c}$$

$$h_4 : L = \frac{\mu_0 N^2 h_4^2}{3b(b+c)} \left[\sec^2 \theta + 2 \tan \theta \right]_0^{\tan^{-1} (b-c)/h_3} \quad (5.25)$$

If the expressions of inductance for the regions h_2 and h_3 above are compared with the equation (5.8) it is seen that the expressions are the same. This means that if h_2 and h_3 in equation (5.25) are the same as those in equation (5.8) both the upper and the lower bounds have the same value. This is not unexpected as for the non-conducting regions where the fields have been assumed constant and known everywhere both the variations in the flux density and in the magnetic potential simply give the same results.

The upper bound of the slot inductance L_+ due to the lower winding is given by the sum of the inductances in equation (5.25). Substituting the various values of the slot dimensions into equation (5.25) we can obtain the upper bound of the slot leakage inductance for the effective slot shape shown in Figure 23, with $t = \frac{1}{2} h_1$ and ϕ conveniently chosen to be 45° ,

$$L_+ = 249.04 \mu_0 \text{ H per unit length} \quad (5.26)$$

The slot length is 34.5" and there are 40 slots per phase. Therefore the leakage reactance per phase is

$$X_s = 3.446 \Omega \text{ per unit length} \quad (5.27)$$

If, however, the effective slot shape of Figure 24 is taken, the upper bound of the slot leakage inductance with $t = h_1$ and $\phi = 45^\circ$,

would be

$$L_+ = 294.45 \mu_0 \text{ H per unit length} \quad (5.28)$$

giving a reactance value of

$$X_s = 4.074\Omega \text{ per unit length} \quad (5.29)$$

5.5 The Improvement of the Upper Bound

Because of difficulties in writing down the equipotential lines in simple algebraic expressions, an improvement of the upper bound in the similar manner as for the lower bound is not possible. Nevertheless we have an upper bound which would be useful in estimating the true value of the slot leakage reactance.

5.6 Comparison between Calculated and Test Results

As stated in section 5.1 the calculated stator slot leakage reactance obtained by the standard design formula is 2.68Ω . The leakage reactance due to other factors (e.g. tooth leakage, overhang, gap, skew and rotor leakage) is 1.76Ω , giving a total calculated value of 4.44Ω as against the test value of 5.25Ω .

Our calculated values of inductance for the case of the upper bound using Figure 23 are:

$$\begin{aligned} \text{Upper bound} &= 3.446\Omega \\ \text{Improved lower bound} &= 3.203\Omega \\ \text{Average slot reactance} &= 3.3245\Omega \end{aligned} \quad (5.30)$$

Due to pitching this value is reduced by a factor of 0.862.

(See Appendix VII for details on the calculation of reduction factors

due to pitching). The average slot reactance is thus $0.862 \times 3.3245\Omega$ = 2.866Ω . To this is added 1.76Ω giving a total leakage reactance of 4.626Ω , 11.9% below the test value.

If, however, the effective slot shape of Figure 24 is used to calculate the upper bound, we have,

$$\begin{aligned}
 \text{Upper bound} &= 4.074\Omega \\
 \text{Improved lower bound} &= 3.203\Omega \\
 \text{Average slot reactance} &= 3.6385\Omega
 \end{aligned} \tag{5.31}$$

Due to pitching this value is reduced to 3.136Ω and adding 1.76Ω to it we obtain a total motor leakage reactance of 4.896Ω which is 6.7% below the test value of 5.25Ω .

5.7 Discussion of Results

In choosing the boundary shape of the slot to be as shown in Figure 23 in which only half the current-carrying region is brought down into a kernel at the centre of the slot bottom, we obtain an average total motor reactance of within 11.9% of the test result. In this case we have assumed that there is a considerable circulation of flux only at the slot bottom. The effects of flux circulation due to finite iron permeability are more extensive in the case of the effective slot shape shown in Figure 24 where the whole of the conducting region is affected. The average calculated reactance is now about 6.7% below the test value.

Our calculated result shows that a considerable amount of magnetic flux circulation is likely to be present in a deep slot surrounded by iron of finite permeability especially when a winding is situated at the

bottom of it. This is the case of the lower high-speed (10 pole) winding. If such effects due to flux circulation is ignored in calculation, a much lower value of the leakage reactance is obtained.

It is thus likely that the assumption that the flux crosses the slot in straight parallel lines is not accurate and acceptable in such cases. However, such effects do not occur or at least do not affect the inductance, as far as the upper low-speed (14-pole) winding is concerned; due to its position in the slot as such. The winding has iron bordering it only on two sides instead of on three as in the case of the lower winding. This means that there is no kernel in the field of the upper winding and the effects of flux circulation are not considerable.

Calculations using the field variational method can be made for the upper 14-pole winding and we find the average motor leakage reactance to be 10.39Ω , less than 1% below the test value of 10.41Ω . The normal design formula gives a calculated value of 9.72Ω . Together with the lower bound of reactance obtained either by the standard methods or the variational method, the upper bound of reactance obtained by taking the effective slot shapes can provide us with a means of making a better estimate of the true slot leakage reactance.

References

1. ALGER, P. L. : 'Induction Machines - their behaviour and uses', Gordon & Breach, New York (1970), Chapter 7, p 199.
2. LIWSCHITZ-GARIK, M. and WHIPPLE, C. C. : 'Electric Machinery', Van Nostrand, New York (1946), Chapter 5, Vol. I, and Chapter 6, Vol. II.
3. RICHTER, R. : 'Elektrische Maschinen', Springer (1950), Vol. IV, pp 161-173.
4. HAMMOND, P. : 'Energy Methods in Electromagnetism', Clarendon Press, Oxford (1981), pp 93-101.
5. LIWSCHITZ-GARIK, M. and WHIPPLE, C. C. : 'Electric Machinery', Van Nostrand, New York (1946), Vol. I, p 65.
6. STEVENSON, Jr. A. R. and PARK, R. H. : 'Graphical Determination of Magnetic Fields : Theoretical Considerations', Paper presented at Winter AIEE Convention, New York, Feb. 1927.

CHAPTER SIXCONCLUSION

To a designer, a method of calculation which provides an upper and a lower bound to a certain parameter of design is useful and helpful. In the design of electrical machines and apparatus, as in any other engineering design, the ability of the designer to predict within known limits the behaviour and performance of his design is important and necessary especially at the present moment of stiff business competitiveness.

The variational method treated in this thesis shows examples of the calculation of electromagnetic system parameters namely the capacitance, inductance and resistance; obtaining the upper and lower bounds of each. The results obtained for the simple configurations used in the examples are in good agreement with those obtained by other methods, be it analytical or numerical. In the calculation of the capacitance of a square tubing, the result obtained are within 1% of the analytically obtained value. The inductance calculated in our example is about 1.1% above the numerically determined value, while the value of resistance we obtain is 1.5% of the value obtained by a finite difference method.

Variational calculations involving system energy in terms of scalar quantities for example the scalar electric potential, are easier to do. Furthermore in such cases the improvement formula obtained in Chapter 3 can be applied to obtain a reasonably substantial improvement of the initial parameter value calculated. Variational calculations involving vector quantities, for example the electric flux density, are

however not as easy to perform and improvement whenever possible is always very slight. In cases where the variational formulation which requires the calculation of system energy, cannot be directly applied, for example in the calculation of the upper bound of inductance in terms of magnetic potential, geometrical approach is adopted. The improvement formula cannot be applied in such cases and for the estimation of the true parameter value we have to use the value obtained without the benefit of such improvement.

In calculating the system energy and in the choice of arbitrary function for the application of the improvement formula, the boundary conditions of the system have to be carefully taken into consideration. Knowledge and insight into the problem to be solved is always helpful especially in determining the correct boundary conditions of the problem. This is especially true if the variational method of calculation is to be applied to 3-dimensional problems. It is perhaps the greatest challenge that the variational method can take up in view of the difficulties involved in 3-dimensional problem solving. Numerical methods developed for tackling 3-dimensional electromagnetic problems are at present still in the early stages. The variational method possesses the inherent capability to be developed for the solution of 3-dimension problems.

The example of the calculation of bounded values for slot leakage reactance shows the possibility of the field variational method to be gainfully applied in machine design problems in conjunction with the well-established standard methods of slot leakage calculation. An alternative method to the standard methods is thus available to the machine designer.

All the examples given have shown that the variational method gives good results and can be suitably and successfully applied to electromagnetic problems.

An important area which needs to be looked into further is the determination of the initial trial function for the various types of problems such as to minimise or maximise the system energy as the case may be. A guide through mathematical analysis, as to the necessary conditions that need to be satisfied for the correct determination of the trial function is necessary particularly in relation to the system equations and the system boundary conditions.

APPENDIX IThe Euler-Lagrange Variational Principle

Let a scalar functional I be expressed in the form

$$I = \int_a^b L(\phi, \phi', x) dx \quad (1)$$

with the boundary points at

$$\phi(a) = \alpha$$

$$\phi(b) = \beta \quad (2)$$

where L is a functional of variables ϕ , ϕ' and x and ϕ' is the first derivative of ϕ with respect to x .

Let L be differentiable up to the second derivative and the derivatives are continuous within the region a to b . See Figure 1.

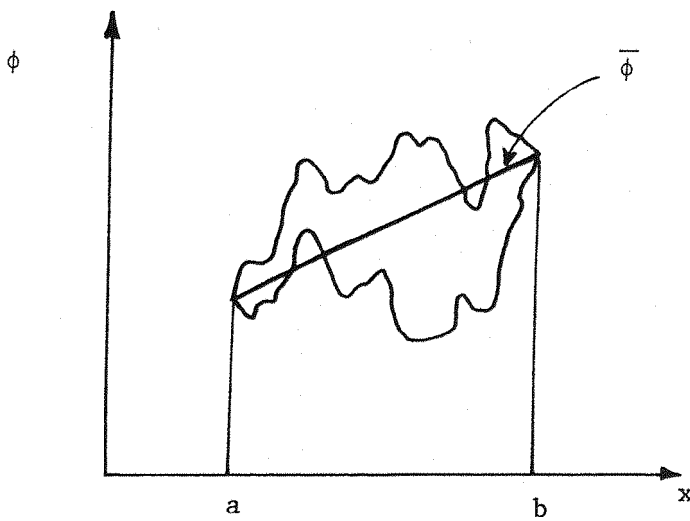


Figure 1 Variations of ϕ between a and b

If I is stationary (maximum, minimum or saddle point) at $\bar{\phi}$, let us consider a small variation $\alpha\psi$ about $\bar{\phi}$, such that

$$\phi = \bar{\phi} + \alpha\psi \quad (3)$$

where α is a constant, ψ an arbitrary function of x .

In order that equation (2) be satisfied, we have at the boundary, such that,

$$\psi(a) = \psi(b) = 0 \quad (4)$$

The functional I for variations about $\bar{\phi}$ is given by,

$$I(\bar{\phi} + \alpha\psi) = I(\bar{\phi}) + \delta I(\bar{\phi}, \alpha\psi) + \delta^2 I(\bar{\phi}, \alpha\psi) + \dots \quad (5)$$

and the first variation of I is,

$$\delta I = \alpha \int_a^b \psi \left[\frac{\partial L}{\partial \phi} \right]_{\bar{\phi}} + \psi' \left[\frac{\partial L}{\partial \phi'} \right]_{\bar{\phi}} dx \quad (6)$$

Integrating equation (6) by parts and using equation (4) for the boundary conditions we obtain,

$$\delta I = \alpha \int_a^b \psi \left\{ \frac{\partial L}{\partial \phi} - \frac{d}{dx} \left(\frac{\partial L}{\partial \phi'} \right) \right\}_{\bar{\phi}} dx \quad (7)$$

The stationarity of I requires that its first variation should vanish. Equation (7) therefore should become zero. Since ψ is an arbitrary function in the region, it follows that the necessary condition for a stationary I is

$$\left\{ \frac{\partial L}{\partial \phi} - \frac{d}{dx} \left(\frac{\partial L}{\partial \phi'} \right) \right\}_{\bar{\phi}} = 0 \quad (8)$$

This is the Euler-Lagrange Differential Equation.

For multivariables $x_1, x_2, x_3, \dots, x_n$, ⁽¹⁾ the Euler-Lagrange Equation is given by,

$$\left\{ \frac{\partial L}{\partial \phi} - \sum_{k=1}^n \frac{\partial}{\partial x_k} \cdot \frac{\partial L}{\partial \phi'_{x_k}} \right\} = 0 \quad (9)$$

The first variation of I therefore vanishes at $\bar{\phi}$ where $\bar{\phi}$ is the solution of the Euler-Lagrange Equation. This is the Euler-Lagrange Variational Principle.

Reference

1. SAGAN, H. : 'Boundary and Eigenvalue Problems in Mathematical Physics', John Wiley & Sons Inc., New York (1961), pp 16-21.

APPENDIX II

The scalar Y and Z functionals of equations (2.22), (2.23), (2.24) and (2.25) in chapter two are:

$$Z = \int_v \bar{\rho}\phi - \frac{1}{2}\epsilon |\underline{E}|^2 dv - \int_s \bar{\rho}_s \phi_s ds \quad (1)$$

$$Z = \int_v \rho\bar{\phi} - \frac{1}{2\epsilon} |\underline{D}|^2 dv - \int_s \rho_s \bar{\phi}_s ds \quad (2)$$

$$Y = \int_v \frac{1}{2}\epsilon |\underline{E}|^2 dv \quad (3)$$

$$Y = \int_v \frac{1}{2\epsilon} |\underline{D}|^2 dv \quad (4)$$

Consider equation (1) first, where the variation is on the potential ϕ with the charges $\bar{\rho}$ and $\bar{\rho}_s$ fixed.

Let

$$\begin{aligned} L &= \frac{1}{2}\epsilon |\underline{E}|^2 - \bar{\rho}\phi \\ &= \frac{1}{2}\epsilon |\underline{\phi}'|^2 - \bar{\rho}\phi \end{aligned} \quad (5)$$

where

$$\underline{\phi}' = \nabla\phi = -\underline{E} \quad (6)$$

$$\text{and } \lambda = \bar{\rho}_s \phi_s \quad (7)$$

For stationary Z it is required that its first variation should vanish, thus,

$$\delta Z = \delta \int_V L \, dv + \delta \int_S \phi \, ds = 0 \quad (8)$$

Variation in the volume potential ϕ makes the second term zero since ϕ_s is the value of ϕ evaluated at the surface and ℓ is a constant with respect to ϕ . Applying the Euler-Lagrange Equation,

$$\frac{\partial L}{\partial \phi} - \frac{\partial}{\partial r} \left(\frac{\partial L}{\partial \phi'} \right) = 0 \quad (9)$$

to equation (5) gives,

$$-\bar{\rho} - \frac{\partial}{\partial r} (\epsilon \phi') = 0 \quad (10)$$

or rewriting for the space operator⁽¹⁾ and using equation (6),

$$-\bar{\rho} + \underline{\nabla} \cdot \underline{\epsilon E} = 0 \quad (11)$$

Using the relationship $\underline{\rho} = \underline{\epsilon E}$, equation (11) becomes

$$\underline{\nabla} \cdot \underline{D} = \bar{\rho} \quad (12)$$

which together with equation (6) are the system differential equations.

Equations (2), (3) and (4) can be similarly treated and we find that the Euler-Lagrange equations in each case are the system differential equations.

Reference

1. LANDAU, L. D. and LIFSHITZ : 'Mechanics and Electrodynamics', Vol. I., Pergamon Press, N. York (1972), p 155.

APPENDIX III

```

***SCIENTIFIC JOBBER B50*** STARTJOB 1 TEEFOU3,KUALALUM

```

```

11 JUE(JU1TAPE#1:TEFOU3,KUALALUM,LINE#250U) H =  $\frac{1}{2}k_3 + k_3 \cdot \delta^2 r^2 \delta^2 + j(B_3 + B_3 \cdot \delta^2 + B_3 \cdot \delta^2)$ 

```

```

110NTR4

```

```

COMPILE,OPTIONS,CHECK,AB

```

EDINBURGH FORTRAN(G) COMPILER VERSION 50

```

1 PROGRAM NAME
2 REAL INDUCTANCE
3 EXTERNAL F1,F2,F3,F4,F5,F6,F7,F8,F9,F10,F11,F12,F13,F14,F15,F16
4 EXTERNAL S1,S2,S3,S4
5 EXTERNAL SHESSJ
6 DIMENSION R(X,X),H(X)
7 COMMON /A/ SO
8 COMMON /H/ S
9 COMMON /C/ B
10 C
11 C BODY CURRENT VARIATIONAL PROBLEM
12 C
13 C SD I SKIN DEPTH
14 C
15 C
16 SD = 1.0
17 N = 6
18 N = N
19 C FOR VARIATIONS IN ALPHA 2
20 CALL TEGRA (F1)
21 R(1,1) = S
22 CALL TEGRA (F2)
23 H(2,1) = S
24 H(2,2) = S
25 C FOR VARIATIONS IN ALPHA 3
26 CALL TEGRA (F3)
27 H(1,2) = S
28 H(4,1) = S
29 CALL TEGRA (F4)
30 H(2,2) = S
31 CALL TEGRA (F5)
32 H(3,1) = S
33 CALL TEGRA (F6)
34 CALL TEGRA (F7)
35 R(3,2) = S
36 CALL TEGRA (F8)
37 R(4,2) = S
38 CALL TEGRA (F9)
39 H(1,3) = S
40 CALL TEGRA (F10)

```

USGS

UNIVERSITY OF
SOUTHAMPTON
COMPUTING
SERVICE

```

40      R(2,3) = S
CALL TEGRA (F11)
41      R(1,4) = S
CALL TEGRA (F12)
42      R(2,4) = S
CALL TEGRA (F13)
43      R(3,3) = S
CALL TEGRA (F14)
44      R(4,3) = S
CALL TEGRA (F15)
45      R(3,4) = S
CALL TEGRA (F16)
46      R(4,4) = S
47      WRITE (6,119)
48      WRITE (6,111) ((R(I,J),I=1,4),J=1,N)
49      FORMAT (1X,4F10.5)
50      111  FORMAT (1X,4F10.5)
51      EVALUATING THE SOURCE MATRIX
52      CALL TEGRA (S1)
53      B(1) = S
54      CALL TEGRA (S2)
55      B(2) = S
56      CALL TEGRA (S3)
57      B(3) = S
58      CALL TEGRA (S4)
59      B(4) = S
60      WRITE (6,112) (B(I),I=1,N)
61      WRITE (6,113) VALUES OF SOURCE MATRIX
62      CALL SOLUT (S,B,N,X)
63      WRITE (6,120) (B (J),J=1,NX)
64      WRITE (6,121) (B (J),J=1,NX)
65      WRITE (6,122) (B (J),J=1,NX)
66      WRITE (6,123) THE VALUES OF UNKNOWN A2A3,B2,B3 ARE
67      CALL TEGRA(S)
68      RESISTANCE = S
69      CALL TEGRA(S)
70      INDUCTANCE = RESISTANCE * 2.0
71      WRITE (6,124) INDUCTANCE
72      WRITE (6,125) RESISTANCE
73      110  FORMAT (1X,2F10.5)
74      400  FORMAT (1X,2F10.5)
75      401  FORMAT (1X,2F10.5)
76      STOP
77      END
78
79      05      C
80      06      C
81      07      C
82      08      SUBROUTINE TEGRA(F)
83      09      COMMON /B/ S
84      110  C
85      111  TO INTEGRATE FUNCTION F FROM A TO B
86      112  C
87      113  A = 0.0
88      114  B = 2.0
89      115  N = 10
90      116  S = 0.0
91      117  WRITE (6,111) N,A,B
92      118  11  FORMAT (1X,2F10.5)
93      119  1  NO OF INTEGRATION STEPS = 115
94      120  1  INTERVAL FROM F3.1, TO F3.1
95      121  S1 = 0.0
96      122  H = (B-A)/N
97      123  SU = F (A) + F (H)

```

UNIVERSITY OF
SOUTHAMPTON
COMPUTING
SERVICE

USGS

```

103      NUN = N = 1
104      DO 100 1=1,NUN
105      100      S1 = S1 + F  (A+I*H)
106      S1 = S1 * 2
107      SHALF = U,U
108      E = 0.0
109      DO 200 1=1,N
110      E = (I - U)*H
111      200      SHALF = SHALF + F  (A+E)
112      SHALF = 6.*SHALF
113      S = H*(S1+SHALF)/6
114      WRITE (0,12) S
115      12      FORMAT (1X, ' VALUE OF INTEGRATION = ', F20.10)
116      RETURN
117      END
118
119
120      C
121      C      SUBROUTINE SOLUT(A,B,N,NX)
122      C      DIMENSION A(0, B(0, B(0, B(0,
123
124      C
125      C      SOLUTION OF K LINEAR EQUATIONS
126      C      SOLUTION OF LINEAR EQUATIONS BY THE GAUSS
127      C      ELIMINATION METHOD PROVIDING FOR INTERCHANGING OF ROWS
128      C      WHEN DIAGONAL COEFFICIENT IS ZERO
129
130      C
131      C      A : SYSTEM MATRIX
132      C      B : ORIGINALLY THE SOURCE MATRIX. FINALLY THE UNKNOWN COLUMN
133      C      N : NUMBER OF UNKNOWNS
134      C      NX : DIMENSION OF MATRIX A
135      C      ELEMENTS OF MATRIX A
136      C      (1,1)  (3,1)  (6,1)
137      C      (1,2)  (2,2)  (5,2)
138      C      (1,3)  (2,3)  (4,2)
139      C      AND SO ON
140
141      C      DO 100 K=1,N
142      C      WRITE (6,113)
143      C      WRITE (6,111) ((A(I,J), I=1,6), J=1,N)
144      C      111      FORMAT (1X,
145      C      113      FORMAT (1X, ' MATRIX VALUES A(I,J) ARE ', F10.5)
146      C      N1 = N-1
147      C      DO 100 K=N1
148      C      K=K+1
149      C      A(K,K)
150      C      WRITE (0,110) C
151      C      IF ( AHS(C) = 0.0000001 ) 1,1,3
152      C      1,1      DO 1 J=K1,N
153      C      1,3      C      TRY TO INTERCHANGE ROWS
154      C
155      C      IF ( AHS(A(J,K)) = 0.00001 ) 1,1,5
156      C      1,5      S  DO 6 L=K,N
157      C      C  A(L,K)
158      C      6      WRITE (0,110) C
159      C      A(L,J)  = C
160      C      L = M(K)
161      C      M(K)  = C
162      C      WRITE (0,110) C
163      C      H(J)  = C
164      C      C  A(X,J)
165

```

```

166      WRITE (6,101) C
167      GO TO 3
168      7  CONTINUE
169      8  WRITE (6,2) K
170      2  FORMAT ('***** SINGULARITY IN ROW ',I5)
171      0  D = 0.0
172      GO TO 300
173      C
174      C  DIVIDE ROW BY DIAGONAL COEFFICIENT
175      C
176      3  C = A(I,K)
177      WRITE (6,102) C
178      0  DU 4  J=K+1,N
179      4  A(I,J) = A(I,J)/C
180      0  C
181      (K) = B(K)/C
182      WRITE (6,355) (H (J) , J=1,NX)
183      C  ELIMINATE UNKNOWN X(K) FROM ROW I
184      C
185      DO 101 K=1,N
186      C=A(I,K)
187      WRITE (6,410) C
188      DU 9  J=K+1,N
189      IF L.ARS(C,A(K,J))=H(0,0,0,0,1) , 100,100,9
190      9  A(I,J) = A(I,J)/A(K,J) = C
191      10  B(I,J) = B(I,J)/A(K,J) = B(K)
192      WRITE (6,355) (H (J) , J=1,NX)
193      100  CONTINUE
194      C
195      C  COMPUTE LAST UNKNOWN
196      C
197      101  IF L.ARS(A(N,N)) = 0.0000012 , 100,101
198      101  B(N) = H(N)/A(N,N)
199      WRITE (6,355) (H (J) , J=1,NX)
200      C
201      C  APPLY BACK SUBSTITUTION TO FIND OTHER UNKNOWN
202      C
203      C
204      DO 200 L=2,N
205      K=N-L
206      K1= K + 1
207      DU 200 J=K+1,N
208      200  B(K) = H(K) - A(K,X)*B(J)
209      C
210      WRITE (6,355) (H (J) , J=1,NX)
211      200  FORMAT (1X,ANSWER IS , 6F10.5)
212      355  FORMAT (1X, VALUES OF ALL NOW , 6F10.5)
213      C
214      C  COMPUTE VALUE OF DETERMINANT
215      C
216      200  D = 1.0
217      200  DU 1=1,N
218      200  0 = D*A(1,1)
219      200  WRITE (6,347) 0
220      347  FORMAT (1X, DETERMINANT IS , 6F10.5)
221      410  FORMAT (1X, VALUE OF C IS , F10.5)
222      300  RETURN
223      END
224      C
225      C  FUNCTION S1(X)
226      COMMON /A/ S0
227      S1 = (S0-X)/2.0/SD
228      RETURN
229      END

```

५०

UNIVERSITY OF
SOUTHAMPTON
COMPUTING
SERVICE

USGS

```

291  FUNCTION S2(X)
292  COMMON /A/ SD
293  S2 = -(4.0*SD*x**2+5.0*x**4+2.0*x**6)/6.0*SD
294  RETURN
295  END

296  FUNCTION S3(X)
297  COMMON /A/ SD
298  S3 = -(1.0*x/2.0*SD)*(X**2+2.0*SD*x)/SD**2
299  RETURN
300  END

301  FUNCTION S4(X)
302  COMMON /A/ SD
303  S4 = -(1.0*x/2.0*SD)*(X**5+6.0*x*SD*x**2+2*x**4)/SD**4
304  RETURN
305  END

306  FUNCTION F1(X)
307  COMMON /A/ SD
308  F1 = 4.0*U*(SD*x)**2
309  RETURN
310  END

311  FUNCTION F2(X)
312  COMMON /A/ SD
313  F2 = 2.0*U*(SD*x)*(4.0*SD*x**2+5.0*x**4)
314  RETURN
315  END

316  FUNCTION F3(X)
317  COMMON /A/ SD
318  F3 = 2.0*(SD*x)*(4.0*x*SD*x**2+1.0*x**4)
319  RETURN
320  END

321  FUNCTION F4(X)
322  COMMON /A/ SD
323  F4 = (4.0*x*SD*x**2+5.0*x**4)**2
324  RETURN
325  END

326  FUNCTION F5(X)
327  COMMON /A/ SD
328  F5 = (X**2+2.0*SD*x)**2*(4.0*x*SD*x**2+1.0*x**4)
329  RETURN
330  END

331  FUNCTION F6(X)
332  COMMON /A/ SD
333  F6 = (X**2+2.0*SD*x)**2*(4.0*x*SD*x**2+1.0*x**4)
334  RETURN
335  END

```

UNIVERSITY OF
SOUTHAMPTON
COMPUTING
SERVICE

USGS

```

211      FUNCTION F 0(X)
212      COMMON /A/ SD
213      F0 = (X+5-6.0*SD**2*X)*(X+2-2.0*SD**2
214      RETURN
215      END

216      FUNCTION F 1(X)
217      COMMON /A/ SD
218      F1 = (X+5-6.0*SD**2*X)*(X+2-2.0*SD**2
219      RETURN
220      END

221      FUNCTION F 2(X)
222      COMMON /A/ SD
223      F2 = (X+5-6.0*SD**2*X)**2
224      RETURN
225      END

226      FUNCTION F 3(X)
227      COMMON /A/ SD
228      F3 = 2.0*SD**2*(X+2-2.0*SD**2
229      RETURN
230      END

231      FUNCTION F 4(X)
232      COMMON /A/ SD
233      F4 = 2.0*SD**2*(X+2-2.0*SD**2
234      RETURN
235      END

236      FUNCTION F 5(X)
237      COMMON /A/ SD
238      F5 = 2.0*SD**2*(X+2-2.0*SD**2
239      RETURN
240      END

241      FUNCTION F 6(X)
242      COMMON /A/ SD
243      F6 = 2.0*SD**2*(X+2-2.0*SD**2
244      RETURN
245      END

246      FUNCTION F 7(X)
247      COMMON /A/ SD
248      F7 = 2.0*SD**2*(X+2-2.0*SD**2
249      RETURN
250      END

251      FUNCTION F 8(X)
252      COMMON /A/ SD
253      F8 = 2.0*SD**2*(X+2-2.0*SD**2
254      RETURN
255      END

```

USGS UNIVERSITY OF
SOUTHAMPTON
COMPUTING
SERVICE

```

311      FUNCTION F15(X)
312      COMMON /A/ SD
313      F15 = (SD-X)*(4.0*SD**2-3.0*X**2) *2.0
314      RETURN
315      END

316      FUNCTION F16(X)
317      COMMON /A/ SD
318      F16 = (SD-X)*(4.0*SD**2-X.0*X**2)*2.0
319      RETURN
320      END

321      FUNCTION F16(X)
322      COMMON /A/ SD
323      F16 = (4.0*SD**2-3.0*X**2)**2
324      RETURN
325      END

326      FUNCTION SH(X)
327      DIMENSION H(H)
328      COMMON /A/ SD
329      COMMON /C/ H
330      SH = ( U.2*(1.0-X/2.0*SD)+B(1)*(X**2-2.0*SD*X)+B(2)*(X**3-3.0*SD*X**2+0.5*SD**3) )**2
331      1*(X)**2 + (B(3)*(X**2-2.0*SD*X)+B(4)*(X**3-4.0*SD*X**2))**2
332      SH = 2.0*SD**2
333      RETURN
334      END

335      FUNCTION SJ(X)
336      DIMENSION B(H)
337      COMMON /A/ SD
338      COMMON /C/ H
339      SJ = (U.2/SD**2+U*B(1)*(SD-X) + B(2)*(4.0*SD**2-X.0*X**2) )**2
340      1 +(B(3)*2.0*(SD-X) + B(4)*(4.0*SD**2-3.0*X**2))**2
341      RETURN
342      END

CC05 1046 BYTES  HLT + DATA  4761 BYTES
STACK 2552 BYTES  DIAG TABLES  1792 BYTES  TOTAL 17950 BYTES
COMPILEATION SUCCESSFUL

```

PARHOL2 SUBROUTINES FORMED BY CC05

```

NU OF INTEGRATION STEPS = 10 INTEGRATION INTERVAL FROM U.U TO Z.U
VALUE OF INTEGRATION = 2.6666666667
NU OF INTEGRATION STEPS = 10 INTEGRATION INTERVAL FROM U.U TO Z.U
VALUE OF INTEGRATION = 8.0000000000

```


Appendix IV Calculation of Unsaturated Leakage Reactance

Using the Ampere Circuital Law for the region in the conductor:

(Refer to Figure 21).

$$H \times b = \left(\frac{y}{h_1} N \right) I \quad (1)$$

$$\therefore H = \frac{yNI}{h_1 b} \quad (2)$$

The electromagnetic energy,

$$E = \frac{1}{2} \mu_0 b \int_0^{h_1} \frac{N^2 y^2}{h_1^2 b^2} I^2 dy \quad (3)$$

$$= \frac{\mu_0 N^2 I^2 h_1}{6b} \quad (4)$$

Similarly for the regions h_2 and h_3 , the energy for each region is given by:

$$\text{Region } h_2 : E = \frac{\mu_0 N^2 I^2 h_2}{2b} \quad (5)$$

$$h_3 : E = \frac{\mu_0 N^2 I^2 h_3}{2c} \quad (6)$$

The total energy for the slot is the sum of (4), (5) and (6),

$$E_{\text{Total}} = \frac{\mu_0 N^2 I^2}{6} \left[\frac{h_1}{b} + \frac{3h_2}{b} + \frac{3h_3}{c} \right] \quad (7)$$

We need to determine the total flux linkages $N\Phi$ as the imposed source of the flux density B in the slot.

$$N\Phi = LI \quad (8)$$

Using the relationship for the energy in terms of I ,

$$\frac{1}{2} LI^2 = E_{\text{Total}}$$

$$LI = \frac{2E_{\text{Total}}}{I} = \frac{\mu_0 N^2 I}{3} \left[\frac{h_1}{b} + \frac{3h_2}{b} + \frac{3h_3}{c} \right] = N\Phi \quad (9)$$

In the case of variation of B with the source $N\Phi$ kept constant, the relationship involving the Y -functional is

$$\frac{1}{2} \frac{(N\Phi)^2}{L} = Y = E_{\text{Total}}$$

$$\therefore L = \frac{(N\Phi)^2}{2Y} = \frac{\mu_0 N^2}{3} \left[\frac{h_1}{b} + \frac{3h_2}{b} + \frac{3h_3}{c} \right] \text{ per unit length} \quad (10)$$

For the lower 10-pole winding, $h_1 = 2.581"$, $h_2 = 2.507"$, $h_3 = 0.105"$, $b = 0.6"$, $c = 0.153"$, and $N = 6$.

$$\therefore L = 226.703 \mu_0 \text{ Henry per unit length} \quad (11)$$

Taking the slot length as 34.5", we obtain the reactance per phase of 40 slots,

$$X_s = 3.137 \Omega \text{ per phase} \quad (12)$$

For the upper 14-pole winding, $h_1 = 2.137"$, $h_2 = 0.173"$, $h_3 = 0.105"$, $b = 0.6"$, $c = 0.153"$, and $N = 12$,

$$\therefore L = 311.270 \mu_0 \text{ H per unit length} \quad (13)$$

and $X_s = 4.307 \Omega \text{ per phase}$ (14)

Appendix V Improvement of the Lower Bound Value of Inductance

The chosen \underline{B}_c has to satisfy the following conditions:

$$\underline{V} \cdot \underline{B}_c = 0 \quad (1)$$

$$\int \underline{B}_c \cdot d\underline{s} = 0 \quad (2)$$

Let the correct choice of \underline{B}_c be:

$$\underline{B}_c = (y-p)\underline{i} \quad \text{within the conducting region} \quad (3)$$

$$\left. \begin{array}{l} \underline{B}_c = (y-q)\underline{i} \\ \underline{B}_c = (y-q)\underline{i} \end{array} \right\} \quad \text{above the conducting region} \quad (4)$$

where \underline{i} is the unit vector in the x-direction.

The expression of \underline{B}_1 for the three regions are (see equation (2) in Appendix IV,

$$\text{Region } h_1 : \underline{B}_1 = \mu_0 H = \mu_0 \frac{NIy}{h_1 b} \underline{i} \quad (5)$$

$$h_2 : \underline{B}_1 = \mu_0 \frac{NI}{b} \underline{i} \quad (6)$$

$$h_3 : \underline{B}_1 = \mu_0 \frac{NI}{c} \underline{i} \quad (7)$$

The variation on \underline{B}_1 gives,

$$\underline{B}_2 = \underline{B}_1 + \alpha \underline{B}_c \quad (8)$$



$$\text{At optimum (minimum)} \quad \alpha = - \frac{\int_v \underline{B}_1 \cdot \underline{B}_c \, dv}{\int_v |\underline{B}_c|^2 \, dv} \quad (9)$$

$$\text{and} \quad Y_2 = Y_1 - \frac{\frac{1}{2\mu_0} \left[\int_v \underline{B}_1 \cdot \underline{B}_c \, dv \right]^2}{\int_v |\underline{B}_c|^2 \, dv} \quad (10)$$

For each of the regions, the second term on the right hand side of equation (10) is given by:

$$\text{Region } h_1 : \frac{b\mu_0 \int_0^{h_1} \left(\frac{NI}{h_1 b} y \right) (y-p) dy}{\int_v |\underline{B}_c|^2 \, dv} \quad (11)$$

$$h_2 : \frac{b\mu_0 \int_0^{h_2} \left(\frac{NI}{b} \right) (y-q) dy}{\int_v |\underline{B}_c|^2 \, dv} \quad (12)$$

$$h_3 : \frac{c\mu_0 \int_0^{h_3} \left(\frac{NI}{c} \right) (y-r) dy}{\int_v |\underline{B}_c|^2 \, dv} \quad (13)$$

To satisfy equation (2) above, equations (12) and (13) are identically zero. Equation (10) therefore becomes:

$$\begin{aligned}
 Y_2 &= Y_1 - \frac{\frac{1}{2\mu_0} \left[b\mu_0 \int_0^{h_1} \left(\frac{NI}{h_1 b} y \right) (y-p) dy \right]^2}{b \int_0^{h_1} (y-p)^2 dy} \\
 &= Y_1 - \frac{\frac{1}{2} \mu_0 \left[bNI \left(\frac{h_1^2}{3} - \frac{h_1 p}{2} \right) \right]^2}{b \left(\frac{h_1^3}{3} + h_1 p^2 - ph_1^2 \right)} \quad (14)
 \end{aligned}$$

For the lower 10-pole winding, a suitable choice for $p = 1.291$.

With $Y_1 = E_{\text{Total}}$ and all the other values as in Appendix IV equation (14) becomes,

$$Y_2 = 111.034 \mu_0 I^2 \quad (15)$$

From equation (9), Appendix IV,

$$N\Phi = 226.703 I \quad (16)$$

Using the relationship,

$$\frac{1}{2} \frac{(N\Phi)^2}{L} = Y_2$$

$$\therefore L = \frac{(N\Phi)^2}{2Y_2} = 231.435 \mu_0 \text{ Henry per unit length} \quad (17)$$

The length of slot is 34.5" and there are 40 slots per phase. The reactance per phase is

$$X_s = 3.203 \Omega \quad (18)$$

For the upper 14-pole winding, $p = 1.07$. Similar treatment as above gives,

$$L_s = 327.304 \mu_0 \text{ H per unit length} \quad (19)$$

$$\text{and } X_s = 4.529\Omega \text{ per phase} \quad (20)$$

Appendix VI Calculation of the Upper Bound of Slot Leakage Reactance

Consider the region of tooth-neck h_3 : (Refer to Figure 23).

Writing the circuital law for each incremental strip, we obtain

$$H\delta x = \frac{\left(\frac{Nb}{c}\right)\delta x}{b} I = \frac{N}{c} \delta x I \quad (1)$$

$$\therefore H = \frac{NI}{c} \quad (2)$$

The incremental inductance of the strip is

$$\begin{aligned} \delta L &= \frac{\delta(N\Phi)}{I} = \frac{B\delta y \frac{N}{c} dx}{I} \\ &= \frac{\mu_0 N^2 \delta y \delta x}{c^2} \end{aligned} \quad (3)$$

The inductance of one strip is thus,

$$\delta L = \frac{\mu_0 N^2 \delta x}{c^2} \int_0^{h_3} dy = \frac{\mu_0 N^2 h_3 \delta x}{c^2} \quad (4)$$

For the whole region of h_3 :

$$L = \int_0^c \delta L = \frac{\mu_0 N^2 h_3}{c} \quad (5)$$

By similar considerations for the other regions,

$$\text{Region } h_4 : L = \frac{2\mu_0 N^2 h_4^2}{3b(b+c)} \left[\sec^2 \theta \tan \theta + 2 \tan \theta \right]_0^{\tan^{-1} \left(\frac{b-c}{h_4} \right)} \quad (6)$$

$$h_2 : L = \frac{\mu_0 N^2 h_2}{b} \quad (7)$$

$$(h_1 - t) : L = \frac{\mu_0 N^2 (h_1^3 - t^3)}{3h_1^2 b} \quad (8)$$

$$t : L = \frac{\mu_0 N^2 t^2}{3h_1^2 \tan^{-1}(b/2t)} \quad (9)$$

The total inductance of the slot is the sum of the five terms of equations (5), (6), (7), (8) and (9).

For the lower 10-pole winding with $h_1 = 2.581"$, $h_2 = 2.060"$, $h_3 = 0.105"$, $h_4 = 0.447$, $t = h_1/2$, $b = 0.6"$, $c = 0.153"$ and $N = 6$, the evaluation of the five equations gives a slot inductance,

$$L_s = 249.04 \mu_0 \text{ Henry per unit length} \quad (10)$$

giving a slot reactance

$$X_s = 3.446 \Omega \text{ per phase} \quad (11)$$

Alternatively if $t = h_1$, equation (8) becomes zero and the slot inductance is

$$L_s = 294.45 \mu_0 \text{ Henry per unit length} \quad (12)$$

and $X_s = 4.074 \Omega \text{ per phase}$ (13)

For the top 14-pole winding $h_1 = 2.137"$, $h_2 = 0$, $h_3 = 0.105"$, $h_4 = 0.173"$, $t = 0$ and $N = 12$,

$$L_s = 428.760 \mu_0 \text{ H per unit length} \quad (14)$$

and $X_s = 5.933 \Omega \text{ per phase}$ (15)

Appendix VII Calculation of the Reduction Factor due to Pitching of Winding

The slot inductance can be written as

$$L_s = L_T + L_B + 2M \quad (1)$$

where L_T = self inductance of top coil

L_B = self inductance of bottom coil

M = mutual inductance of the two coils

From equation (10) of Appendix IV

$$L_B = \frac{\mu_0}{3} \left(\frac{N}{2}\right)^2 \left[\frac{h_1}{b} + \frac{3(h_1+h_2)}{b} + \frac{3h_3}{c} \right] \quad (2)$$

$$\text{and } L_T = \frac{\mu_0}{3} \left(\frac{N}{2}\right)^2 \left[\frac{h_1}{b} + \frac{3h_2}{b} + \frac{3h_3}{c} \right] \quad (3)$$

where N = total number of turns for the two coils.

Let $I = i \cos \theta$

and $I' = i \cos \phi$

Writing the Ampere Circuital Law in the region above the lower bottom coil, (Refer to Figure 21)

$$H_b = \left(\frac{N}{2}\right) i \cos \phi$$

$$\therefore H = \left(\frac{N}{2b}\right) i \cos \phi \quad (4)$$

The flux linkages due to this field acting on the top coil and the regions above it is given by

$$\text{Flux linkages} = \int_0^{h_1} \left(\frac{Ny}{2h} \right) \mu_0 H dy + \int_0^{h_2} \left(\frac{N}{2} \right) \mu_0 H dy + \int_0^{h_3} \left(\frac{N}{2} \right) \mu_0 H dy$$

(5)

The mutual inductance is therefore

$$M = \frac{\text{Flux linkage}}{i} = \frac{\mu_0 N^2 \cos\phi}{8} \left[\frac{h_1}{b} + \frac{2h_2}{b} + \frac{2h_3}{c} \right]$$

(6)

The total slot inductance from equations (1), (2), (3) and (6) is

$$L_s = \frac{\mu_0 N^2}{4} \left[\frac{5h_1}{3b} + \frac{2h_2}{b} + \frac{2h_3}{c} + \left(\frac{h_1}{b} + \frac{2h_2}{b} + \frac{2h_3}{c} \right) \cos\phi \right]$$

(7)

Evaluating equation (7) with $h_1 = 1.2905"$, $h_2 = 2.507"$, $h_3 = 0.105"$, $b = 0.6"$, $c = 0.153"$, and $N = 6$, gives

$$L_s = (119.825 + 106.92 \cos\phi) \mu_0 \text{ Henry per unit length}$$

(8)

For different values of pitching and hence ϕ we obtain:

Leading Pitch p.u.	1.0	0.83	0.75	0.67	0.50	0.34	0.17	0.0
ϕ	0°	30°	45°	60°	90°	120°	150°	180°
μ_0	226.74	212.42	195.43	173.28	119.825	66.36	27.23	12.91
$\frac{1}{x} = \text{Reduction factor}$	1.0	0.937	0.862	0.764	0.528	0.293	0.120	0.057

APPENDIX VIIIAN IMPROVED FORMULA FOR SLOT LEAKAGE INDUCTANCESUMMARY

The behaviour of induction motors depends to a considerable extent on the leakage inductance. One important constituent of this reactance is the slot leakage. An accurate value of this inductance can be obtained by means of a detailed flux map, but the normal practice in design offices is to use a simple formula containing the slot dimensions. In the paper it is shown that the assumptions of the formulae are consistent with providing a lower bound to the slot inductance. If there is appreciable saturation in the slot walls and especially at the bottom of the slot, it is likely that the lower bound will be a poor approximation to the correct value. It is then desirable to calculate an approximate upper bound and to take the average of the two bounded values. The paper describes how this can be done and suggests a modified design formula. A numerical example is given and compared with test results on a two-winding machine in which the effect can be isolated.

AN IMPROVED FORMULA FOR SLOT LEAKAGE INDUCTANCE

P. Hammond and Y.K.H. Fuad
 Department of Electrical Engineering,
 Southampton University, England

1. INTRODUCTION

Slot leakage is an important component of the leakage reactance of induction motors and has therefore an appreciable effect on the motor behaviour at starting. Although accurate values can in principle be obtained by means of a complete flux map, it is not easy to compute the flux at the iron-air interface. The normal practice in design offices is to use a formula based on the assumption that the flux traverses the slot at right angles to its sides^{1,2}. In general this assumption is borne out in practice, but if there is appreciable flux circulation in the slot there is some doubt. Recently the authors' attention was drawn to test results on a motor which suggested that the design calculation had given too low a value for the slot leakage and it was decided to investigate the basis of the design formula.

2. BOUNDED SOLUTIONS FOR THE SLOT LEAKAGE INDUCTANCE

In a recent book³ one of the authors has shown that any approximate flux plot gives a lower bound to the associated inductance. In physical terms the flux seeks the easiest route and any approximation intro-

duces constraints which reduce the permeance. The value of the calculated inductance rises to the correct value as the accuracy of the flux plot is increased. Consider first unsaturated teeth and assume for simplicity an open slot with parallel sides in which there is a single conductor. Fig. 1 illustrates the simple flux distribution of the design formula and Fig. 2 illustrates a slightly more accurate flux plot⁴. The field in the bottom of the slot is somewhat different, but since it is weak in this region the effect on the inductance is small.

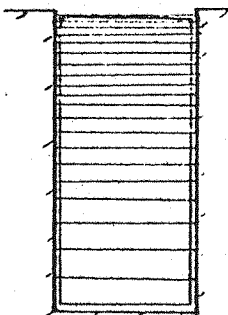


Fig. 1

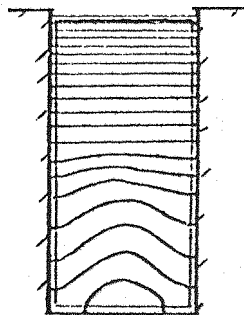


Fig. 2

Fig. 3 illustrates the effect of flux circulation due to finite permeability of slot sides, which is more prominent in the lower parts of the slot. It is clear that because of the curvature of the flux the design formula is less accurate when there is appreciable flux circulation. Since a

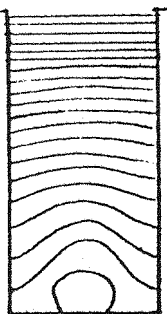


Fig. 3

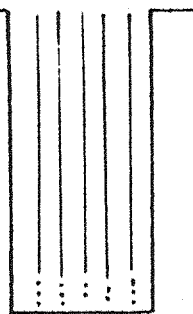


Fig. 4

flux plot provides a lower bound, the motor inductance on test is higher than the calculated value. However, the effect may still be small, because even with finite permeability the flux will still enter the teeth more or less at right angles.

One way of improving the calculation is to improve the flux map, but this is not easy. Another way is to find an upper bound to the solution. In the book³ already mentioned it is shown that such upper bounds can be obtained by modelling the lines of zero field strength. In a region which has no current such lines are equipotentials. Where there is current we can describe them as lines of equal magnetomotive force.

For an unsaturated slot surrounded by infinitely permeable iron we can assume that the slot sides are equipotentials. Fig. 4 shows a potential plot. At the bottom of the slot there is an undetermined region of very weak field. It is interes-

ting to note that the assumption of zero magnetic field strength along the sides of the slot is more demanding than the assumption of horizontal flux lines. The flux will always tend to enter an iron surface more or less at right angles, because the ratio of the tangents of the angles shown in Fig. 5 is equal to the relative permeability μ_r .

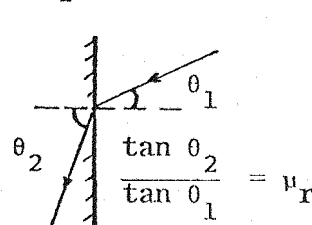


Fig. 5

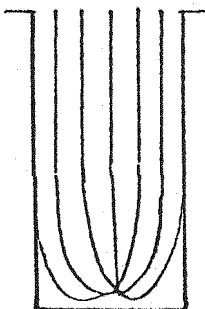


Fig. 6

But this does not mean that there is no field along the iron. This would be true only if μ_r were infinite. It is, therefore, likely that a plot of equipotentials will be more sensitive to the effect of finite permeability.

Fig. 6 shows such a plot and should be compared with Fig. 3. It will be seen that the lines of constant m.m.f. curve towards each other in the bottom of the slot. They converge in a kernel of the field. The effect is to taper the field region and a simple model is given in Fig. 7. The concentration of the field increases the energy and hence the inductance.

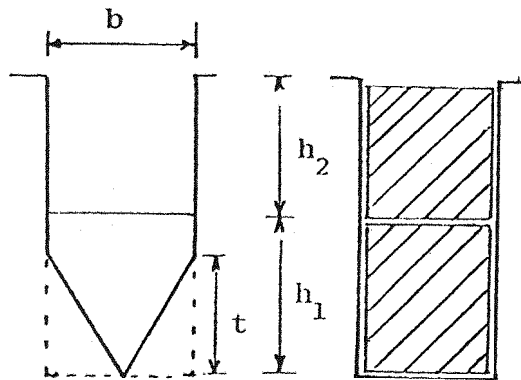


Fig. 7

Fig. 8

Table 1 shows some typical calculations of this effect.

$h_1 = 2.581"$ $h_2 = 2.612"$ $b = 0.6"$	t	Upper Bound Inductance per unit length
	0	$5.787 \mu_o$
	$h_1/4$	$5.812 \mu_o$
	$h_1/2$	$5.973 \mu_o$
	h_1	$7.234 \mu_o$

Table 1

Table 2 shows the averages of the upper and lower bounds and compares these with the lower bounds obtained by means of the usual design formula.

t	Upper Bound Inductance μ_o	Lower Bound μ_o	Average Inductance μ_o
0	5.787		5.787
$h_1/4$	5.812		5.800
$h_1/2$	5.973	$L = \mu_o \left[\frac{h_1}{3b} + \frac{h_2}{b} \right]$	5.880
h_1	7.234	5.787	6.511

Table 2

3. COMPARISON BETWEEN CALCULATED AND TEST RESULTS

Fig. 8 shows a stator slot containing two conductors. These conductors belong to two separate windings and the inductance of the two windings was obtained both by calculation and on test. Fig. 9 shows a simplified slot shape used in calculation. The usual design formula for the lower winding gives a slot leakage reactance of $X = 2.71\Omega$. The upper bound on the assumption of Fig. 9 is given by $X_+ = 3.51\Omega$. The average of X_- and X_+ is $X_{av} = 3.11\Omega$. The total machine leakage reactance was calculated as 4.44Ω but the test value was 5.25Ω . The calculated value is 15.4% below the test value. If the error is due to the calculation of the slot leakage alone, we obtain a calculated value of $(4.44\Omega - 2.71\Omega + 3.11\Omega) = 4.84\Omega$. This is only 7.8% below the test value.

If we use Fig. 10 to estimate the upper bound we obtain $X_+ = 2.97\Omega$ giving an average reactance

$X_{av} = 2.84\Omega$. This makes the total calculated reactance to be 4.57Ω , about 13% below the test value.

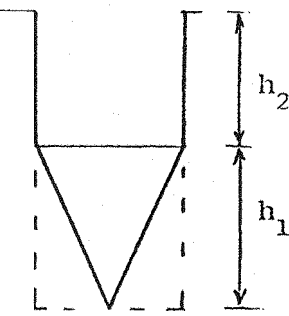


Fig. 9

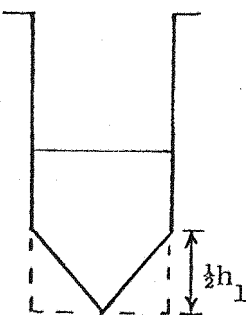


Fig. 10

The total machine leakage reactance due to the winding in the top of the slot was calculated by the usual formula as $X = 9.84\Omega$ and the test value corresponds to $X = 10.41\Omega$. The calculated value is only 5.5% below the test value. For another machine, the design calculated total leakage reactance due to the lower winding was 1.18Ω , about 10% below the test value of 1.31Ω . The slot leakage by the usual formula is given by $X_- = 0.65\Omega$ and the upper bound using Fig. 9 is given by $X_+ = 0.77\Omega$, giving an average of $X_{av} = 0.71\Omega$. If this average value is taken as the slot leakage reactance, we have a calculated value of $(1.18 - 0.65 + 0.71)\Omega = 1.24\Omega$, only 5.3% below the test value. For the upper winding the calculated value of total leakage reactance is 1.41Ω , 7.2% below the test value of

1.52Ω . Thus the usual formula gives a reasonably close estimate of the test value. This is as expected because the upper winding does not experience the effect at the bottom of the slot.

4. CONCLUSION

If there is considerable flux circulation due to finite permeability the slot leakage calculated by the usual design formula is likely to be low. In such cases an improved value can be obtained by calculating an upper bound of the reactance and taking the average. A flux plot always gives a lower bound and a potential plot gives an upper bound.

5. REFERENCES

- (1) Liwschitz-Garik, M.: 'Electric Machinery', Vol. I, Van Nostrand, New York, 1964, pp 64-69.
- (2) Alger, P.L.: 'Induction Machines - Their behaviour and uses', Gordon & Breach, New York, 1970, pp 201-206.
- (3) Hammond, P.: 'Energy Methods in Electromagnetism', Clarendon Press, Oxford, 1981, pp 93-101.
- (4) Stevenson, Jr. A.R., and Park, R.H.,: 'Graphical Determination of Magnetic Fields - Theoretical Considerations', paper at Winter Convention, AIEE, N. York, Feb. 1927.